



南昌大学
NANCHANG UNIVERSITY

观测域医学成像与生成—— 从多分布到多任务

汇报人：官瑜

南昌大学成像与视觉表示实验室 (LIVE)

格物致新 厚德泽人

目录

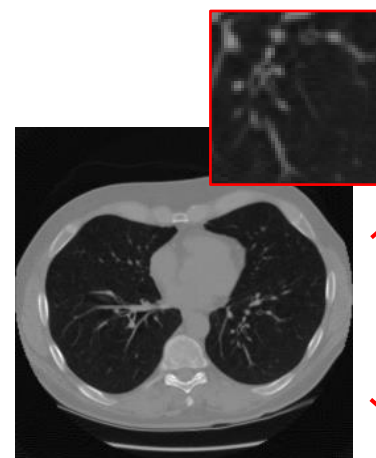


目录

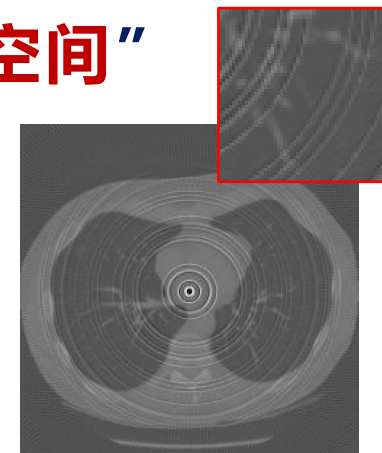
- 01 研究背景**
——从图像域走向原始观测域
- 02 核心突破**
——多分布表征的观测域成像建模
- 03 模型赋能**
——多任务驱动观测域智能生成

研究背景

CT图像域-“可见空间”



原始图像

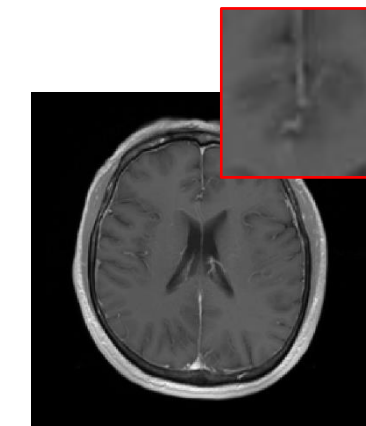


环状伪影图像



几何伪影图像

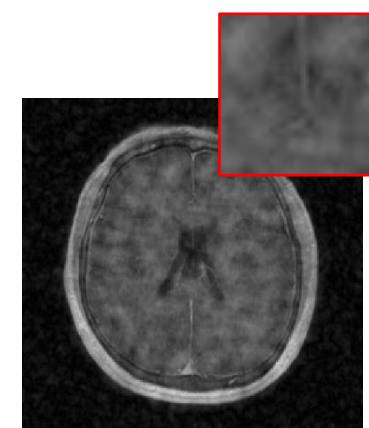
MR图像域-“可见空间”



原始图像



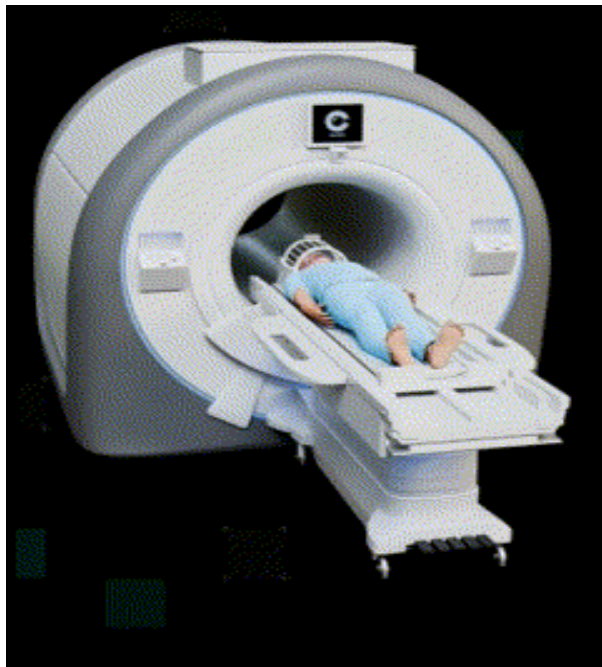
噪声图像



随机欠采图像

研究背景

MRI成像



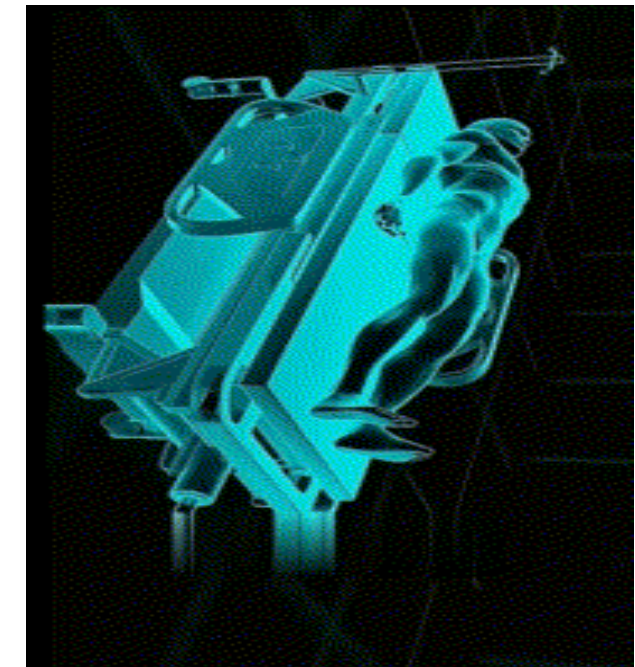
磁化信号
空间频率编码

CT成像



X射线衰减
积分投影

PET成像

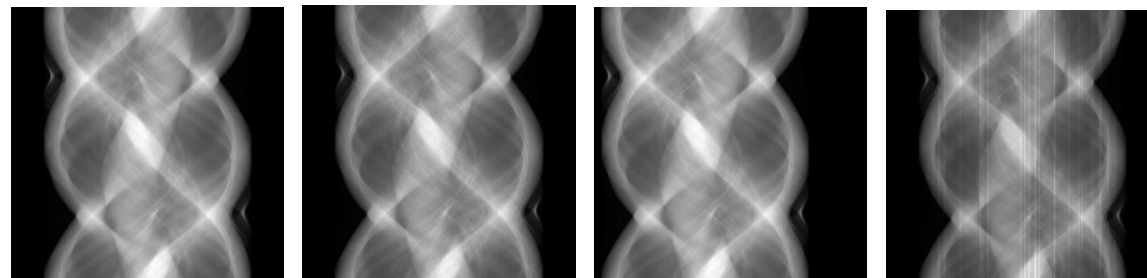


放射性示踪剂
计数投影

研究背景



CT 投影域



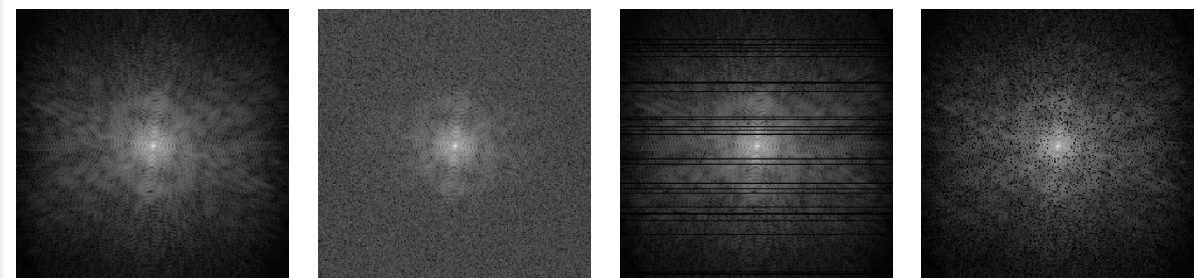
原始信号

噪声信号

偏移信号

伪影信号

K 空间域

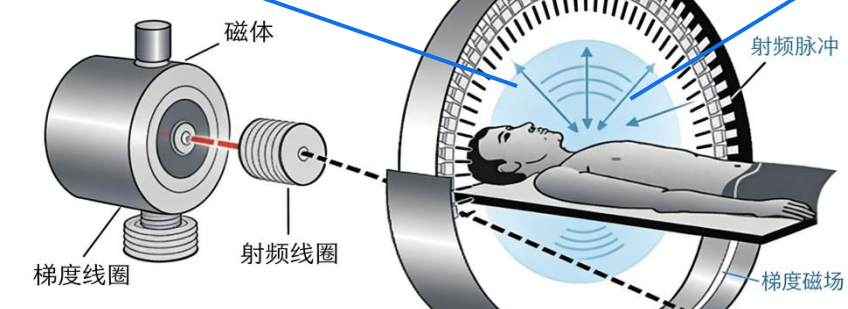
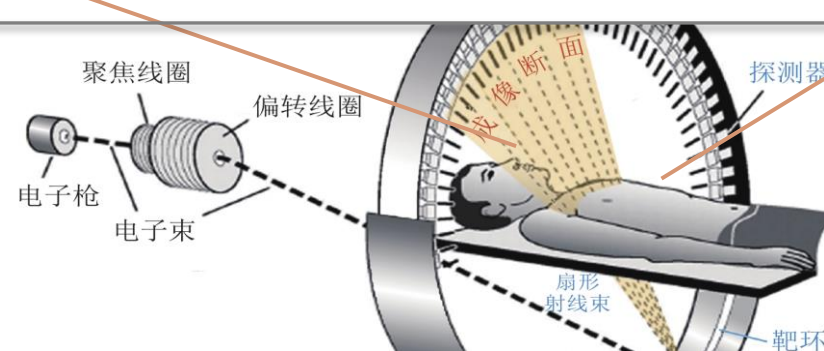


原始信号

噪声信号

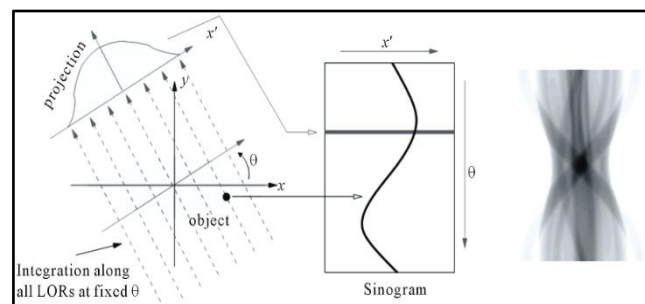
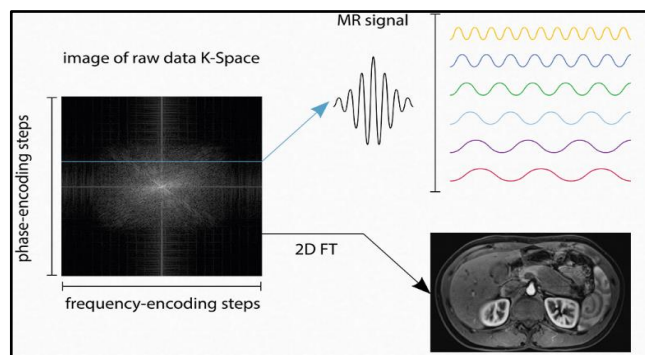
笛卡尔采样

随机采样



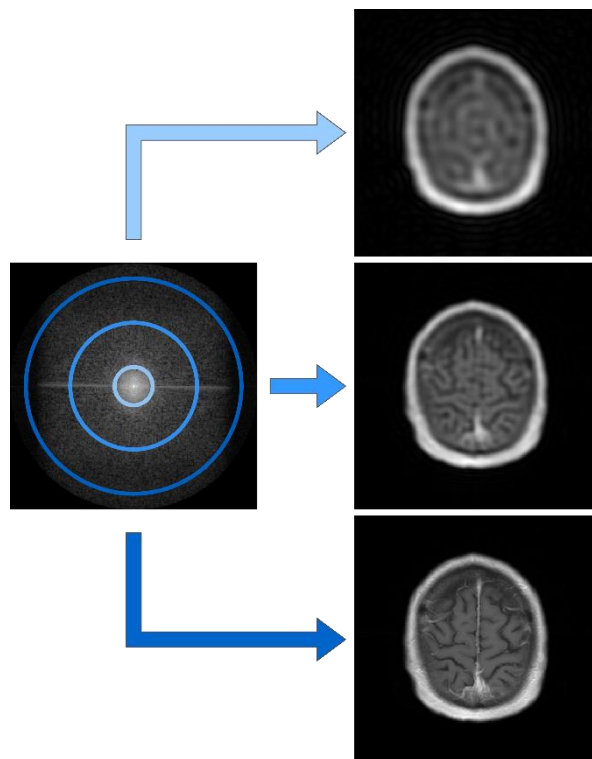
研究背景

物理一致性



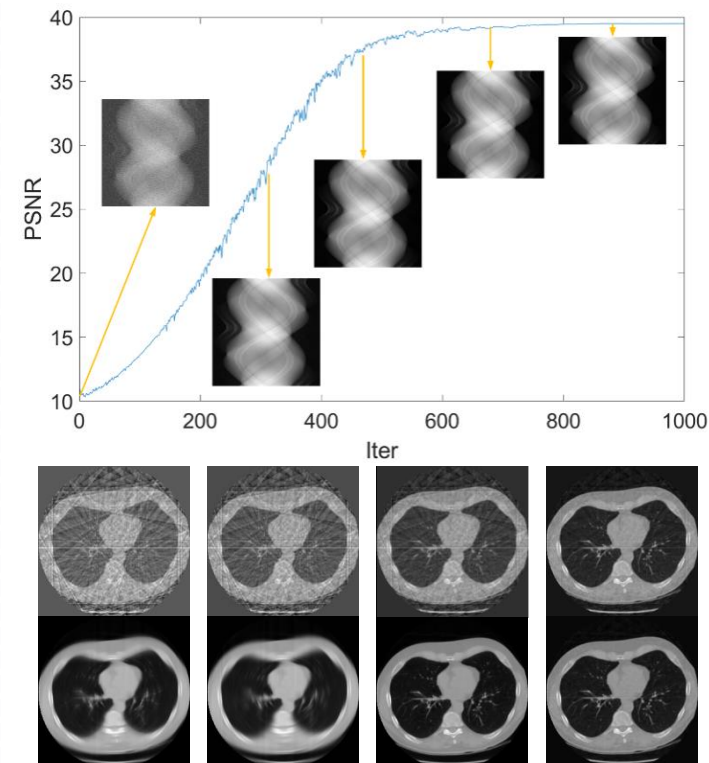
遵循系统采集物理特性
承载完整采样物理信息

全局耦合性



具备卷积和积分特性
单一信号即可表征全局信息

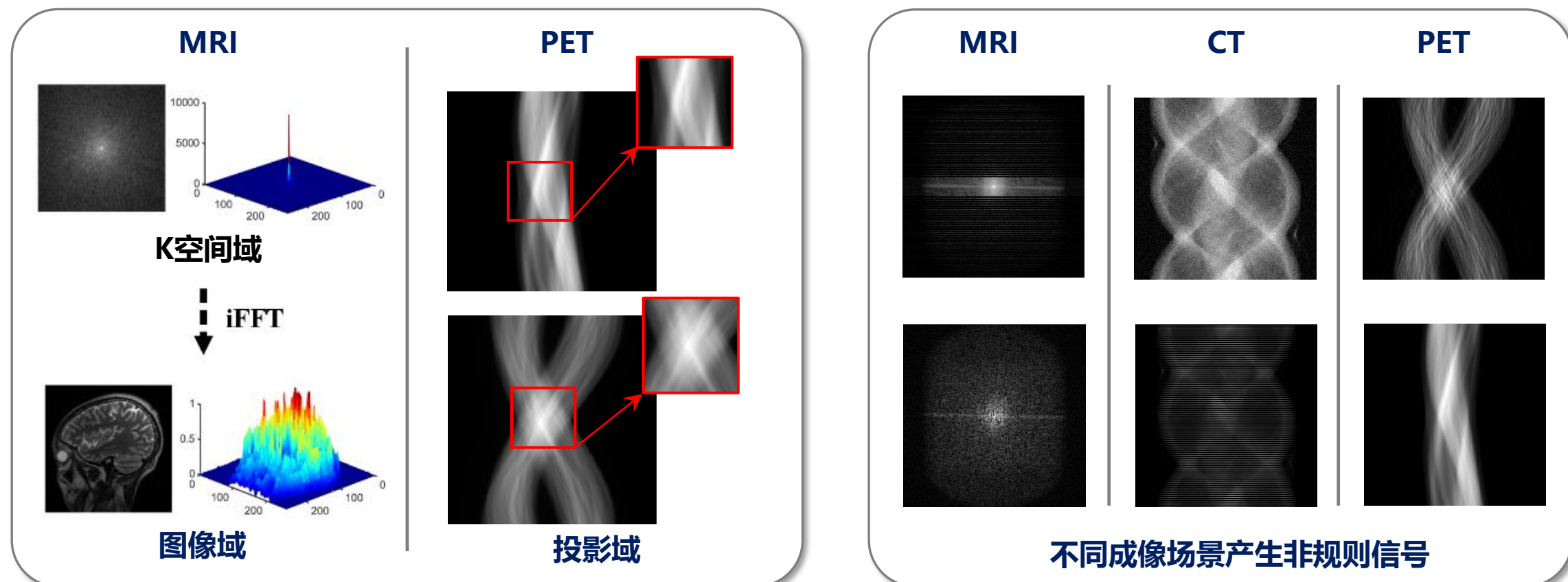
误差可控性



逐信号点估计直接定位误差来源
从源头避免误差累积

研究背景

问题一 非均匀性、非规则性



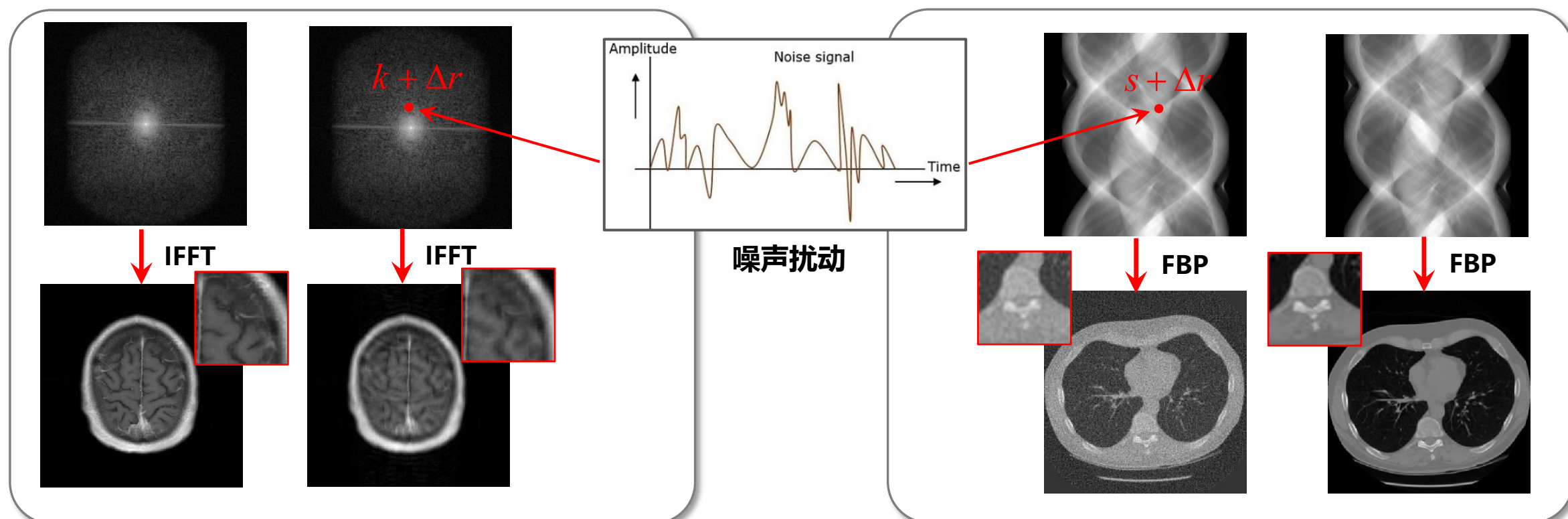
“能量分布非均匀” + “采样结构非规则” → 难以直接学习和稳定建模

研究背景

问题二

“单点偏差” → “全图扰动”

观测域中的每一个采样点均与整个图像域有关，单点偏差会在反演过程中扩散至整个图像域

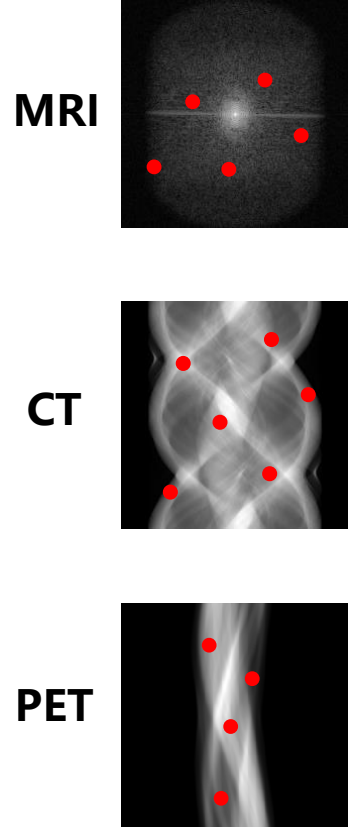


“图像看起来对” → 直接对观测信号进行精确估计！

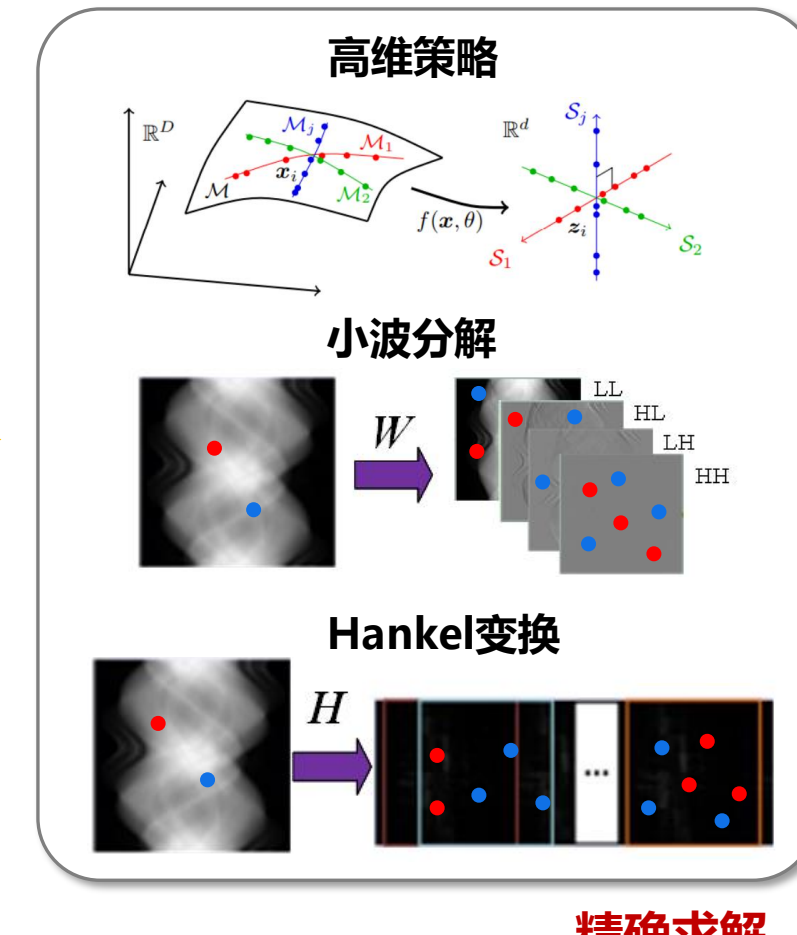
研究内容——关键技术

突破点

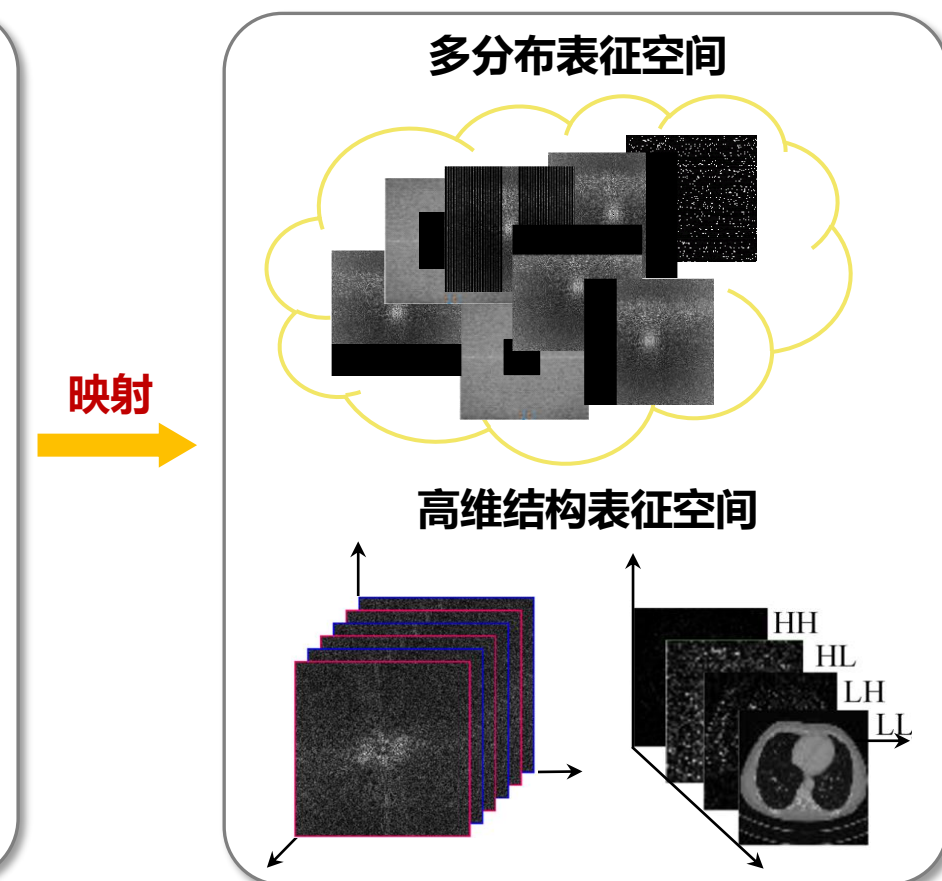
多分布表征——突破生成式学习在观测域成像下的建模壁垒



逐点估计



精确求解



目录



目录

- 01 研究背景**
——从图像域走向原始观测域

- 02 核心突破**
——多分布表征的观测域成像建模

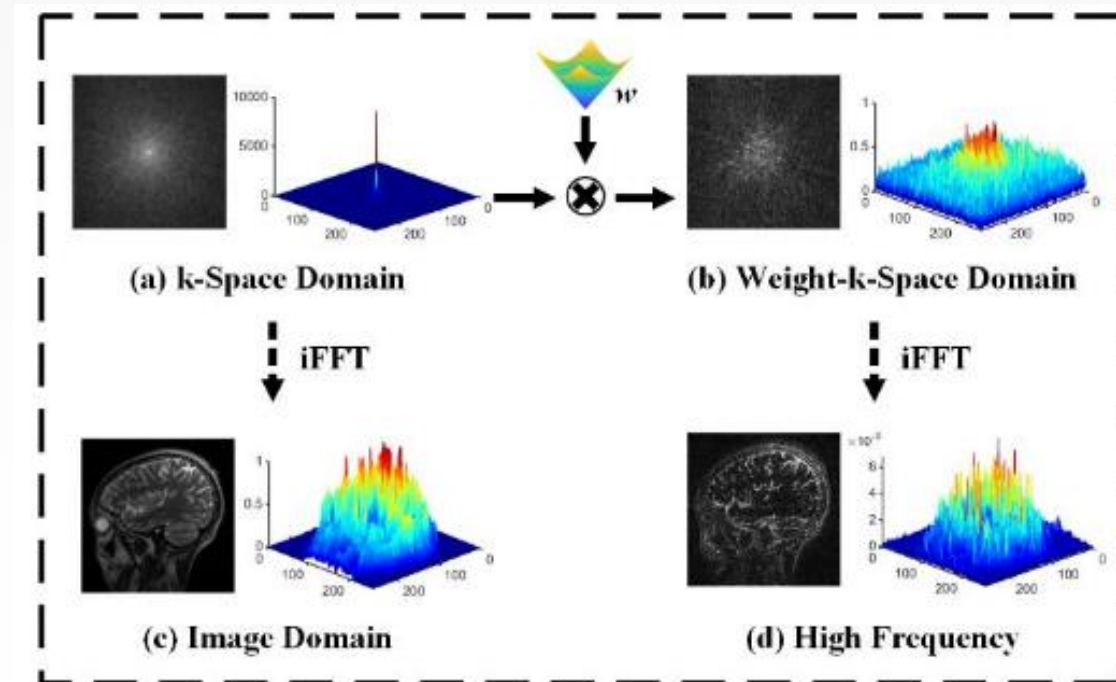
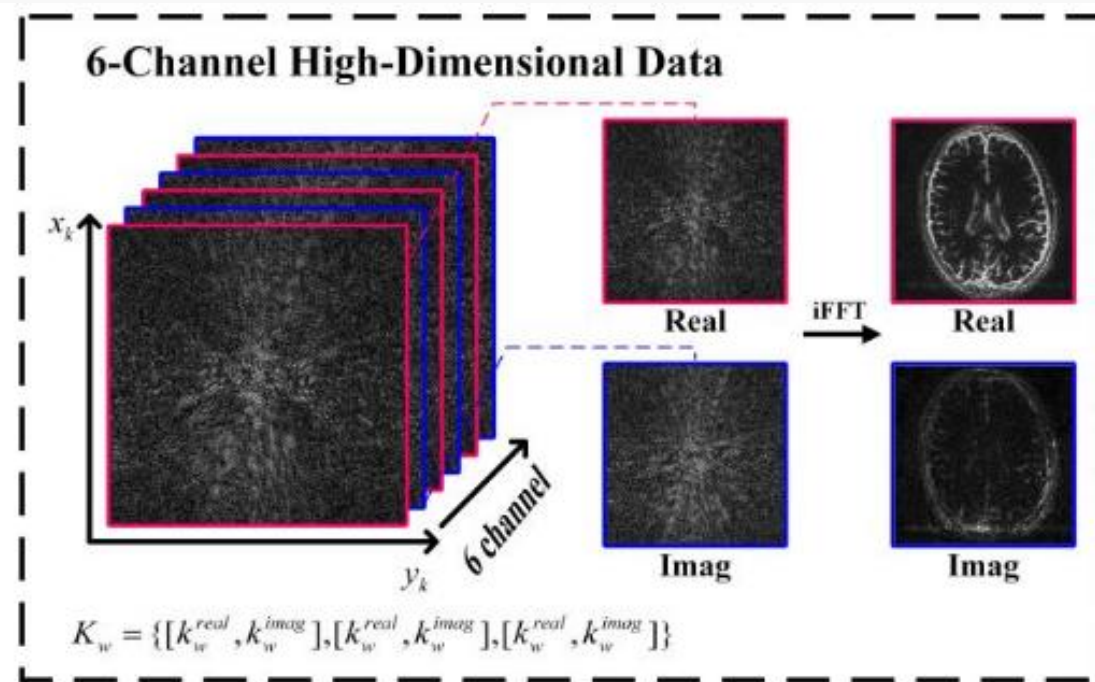
- 03 模型赋能**
——多任务驱动观测域智能生成

研究内容

WKGM

Weight-K-space Generative Model for Parallel Imaging Reconstruction

加权高维并行MRI重建



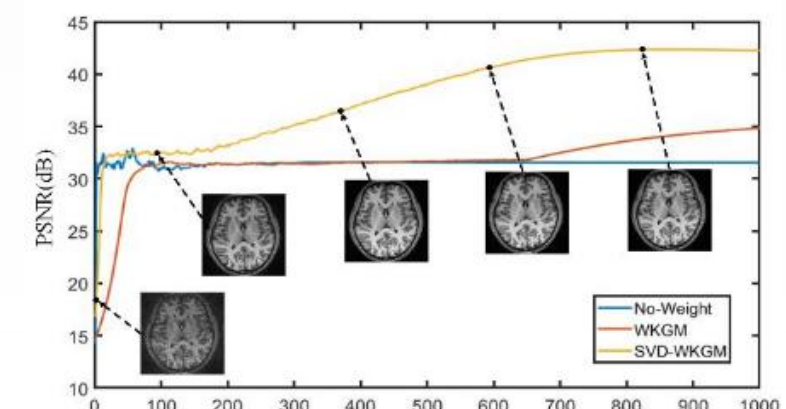
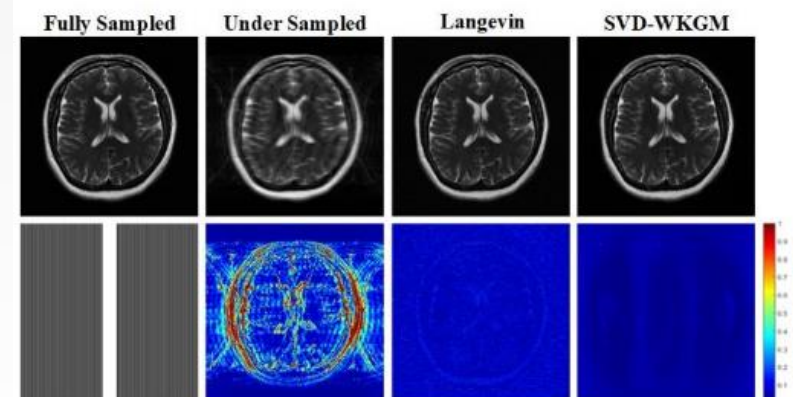
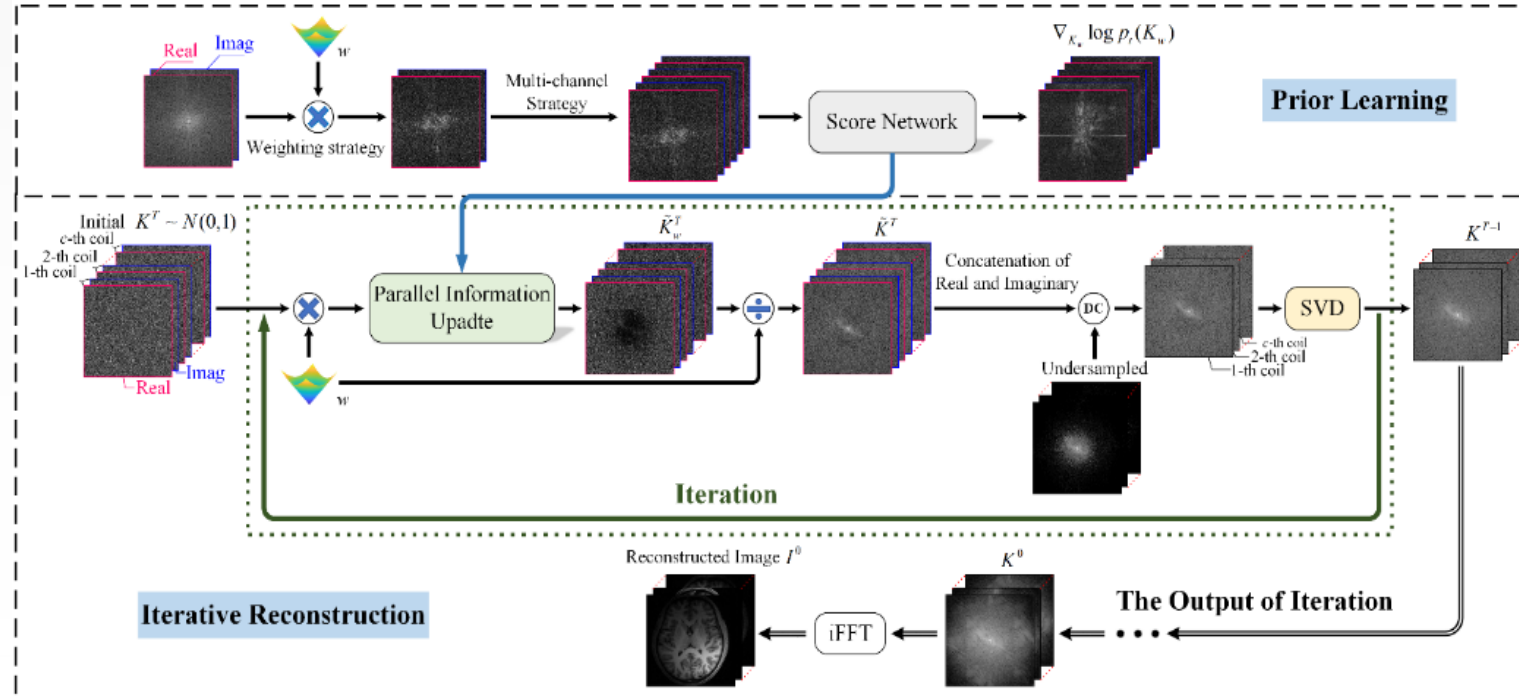
拓展空间维度，学习多线圈数据间的内在相关性，实现无需显式校准的并行成像重建

研究内容

WKGM

Weight-K-space Generative Model for Parallel Imaging Reconstruction

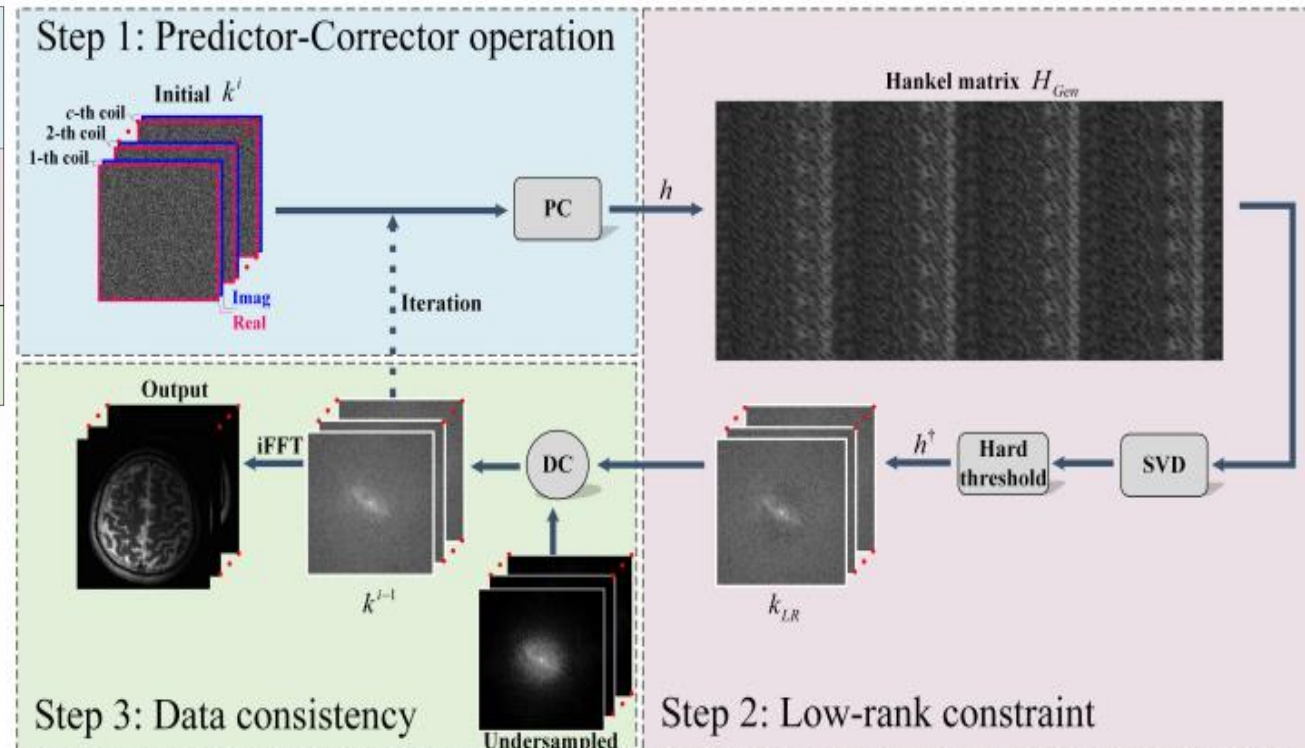
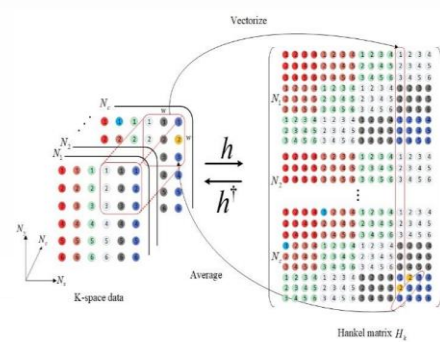
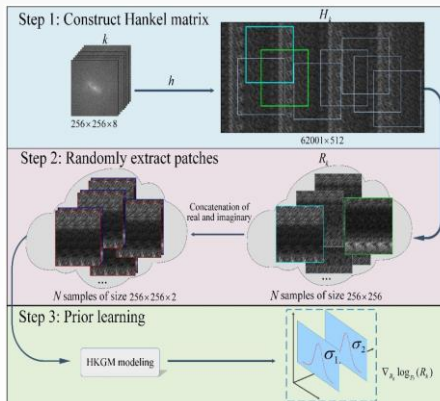
算法流程



研究内容

HKGM One-Shot Generative Prior in Hankel-k-Space for Parallel Imaging Reconstruction

在Hankel化k空间中学习结构化生成先验，实现并行高质量MRI重建



Algorithm 1 HKGM

Training stage

- 1: **Dataset:** the single k-space data
- 2: Construct Hankel matrix $H_k = h(k)$
- 3: Extract patches $\{R_k^i\}_{i=1}^N$ from the matrix
- 4: **Training:** Eq. (10)
- 5: **Output:** Trained $S_\theta(R_k, \sigma)$

Reconstruction stage

- Setting:** N, M
- 1: $H^N \sim N(0, \sigma_f^2 I)$
 - 2: For $i = N - 1$ to 0 do (Outer loop)
 - 3: $\tilde{k}^i \leftarrow \text{Predictor}(k^{i+1}, \sigma_i, \sigma_{i+1})$
 - 4: $H_{Gen}^i \leftarrow h(\tilde{k}^i)$ (Hankel matrix)
 - 5: $[U, \Sigma, V] = \text{SVD}(H_{Gen}^i)$ (Perform SVD)
 - 6: $G^{Th_r}(H_{Gen}^i) = U(Th_r(\text{diag}(\Sigma)))V^\dagger$
 - 7: $\tilde{k}_{LR}^i \leftarrow h^\dagger(G^{Th_r}(H_{Gen}^i))$
 - 8: Update Eq. (22)
 - 9: For $j = 1$ to M do (Inner loop)
 - 10: $\tilde{k}^{i,j} \leftarrow \text{Corrector}(\tilde{k}^{i,j-1}, \sigma_i, \varepsilon_i)$
 - 11: $H_k^{i,j} \leftarrow h(\tilde{k}^{i,j})$ (Hankel matrix)
 - 12: $[U, \Sigma, V] = \text{SVD}(H_k^{i,j})$ (Perform SVD)
 - 13: $Th_r(H_{Gen}^i) = U(Th_r(\text{diag}(\Sigma)))V^\dagger$
 - 14: $\tilde{k}_{LR}^i \leftarrow h^\dagger(Th_r(H_{Gen}^i))$
 - 15: Update Eq. (22)
 - 16: $k^{i,j} \leftarrow \tilde{k}^{i,j}$
 - 17: End for
 - 18: End for
 - 19: $k^{rec} \leftarrow \tilde{k}^0$
 - 20: Return $I_{SOS} = \sqrt{\sum_{c=1}^C |(F^{-1}k_c^{rec})|^2}$

研究内容

HKGM One-Shot Generative Prior in Hankel-k-Space for Parallel Imaging Reconstruction

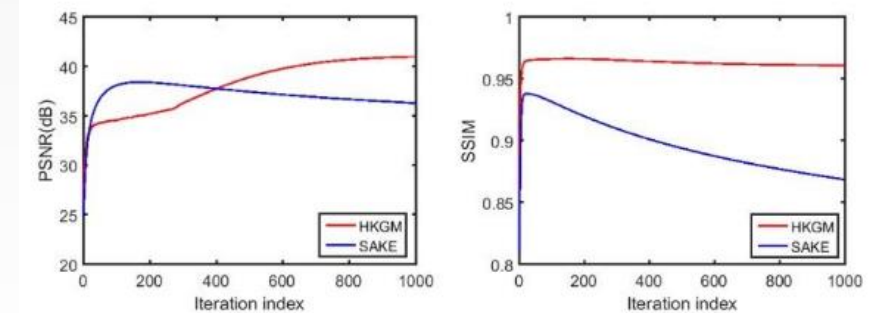
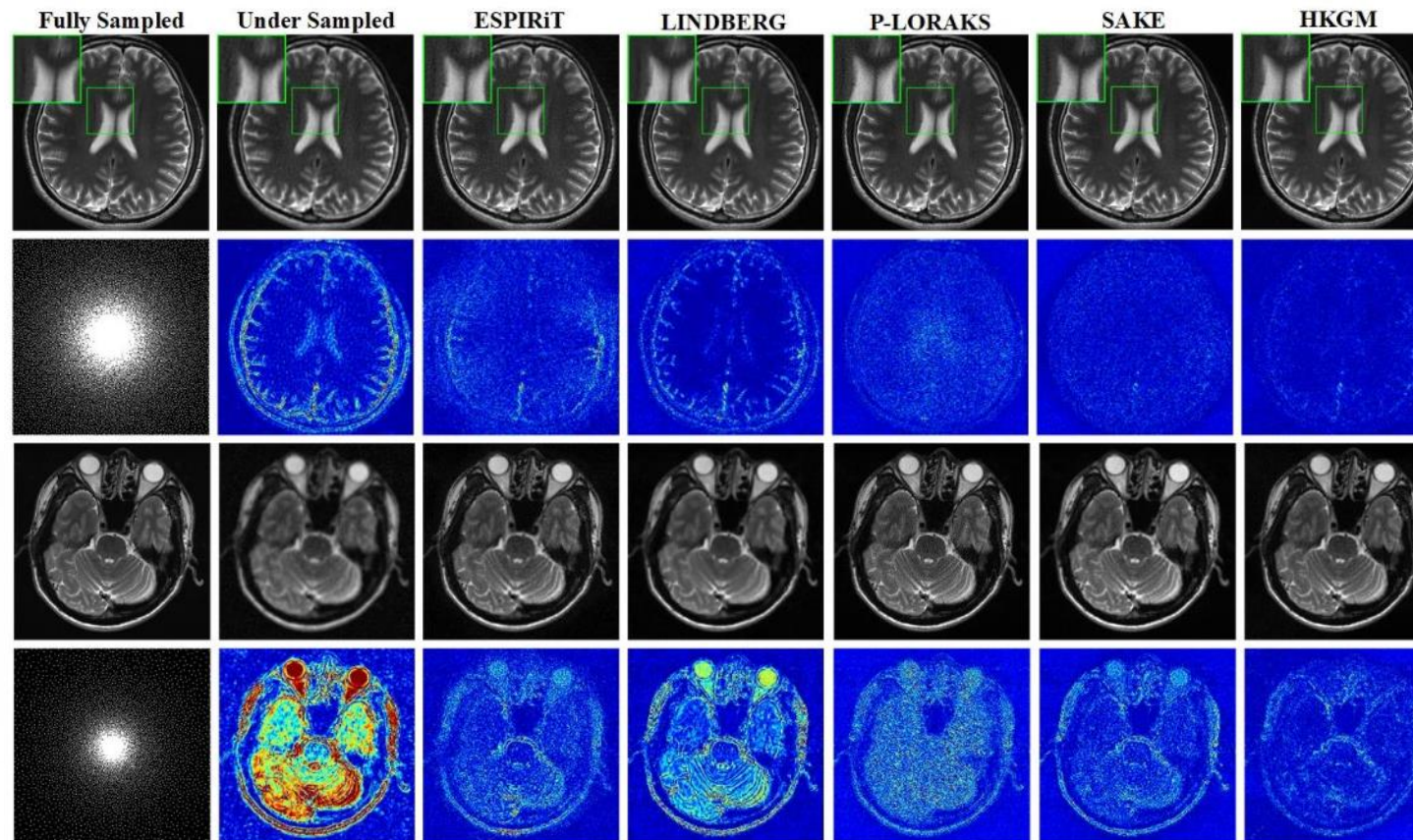


Fig. 10. Convergence curves of SAKE and HKGM in terms of PSNR and SSIM versus iterations when reconstructing the brain image from 1/6 2D random sampled data.

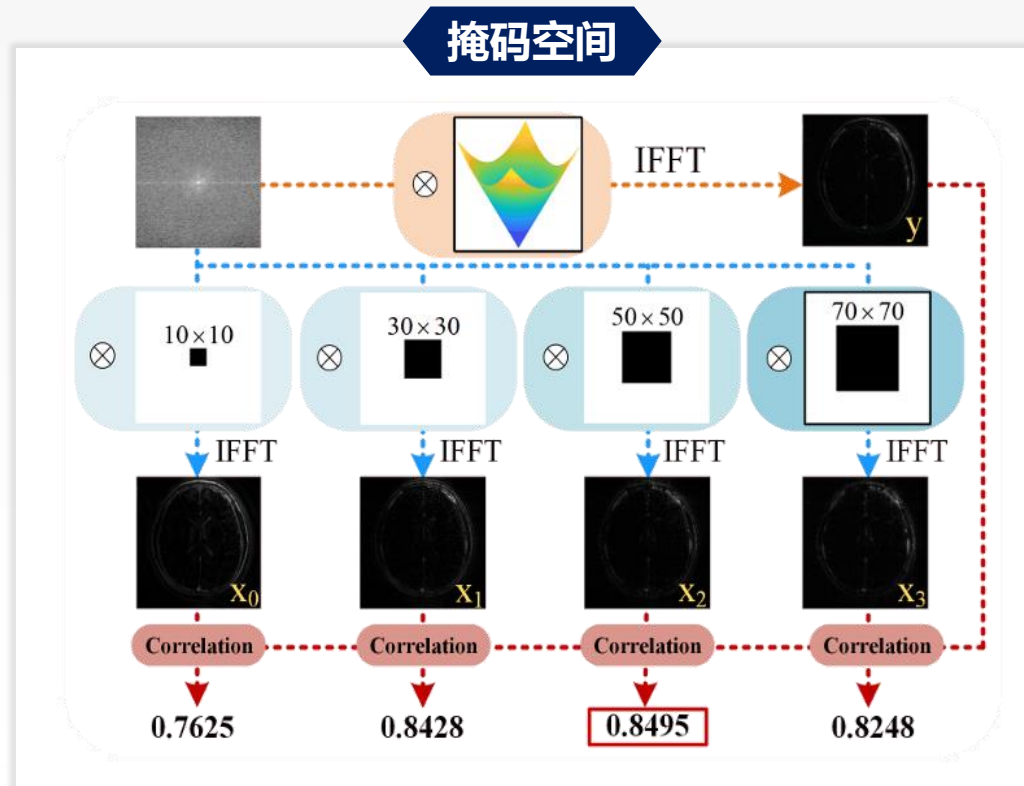
Data in Fig. 6(d)	ESPIRiT	HKGM
Poisson R=4	31.12/0.833	34.76/0.910
Poisson R=10	26.68/0.777	30.54/0.818
2D Random R=4	30.36/0.775	33.87/0.893
2D Random R=6	29.47/0.741	31.76/0.858

研究内容

CM-DM

Correlated and Multi-frequency Diffusion Modeling for Highly Under-sampled MRI Reconstruction

掩码机制驱动的MRI频域多分布构造



迭代算法

Algorithm 1 CM-DM for Iterative Reconstruction

Required: Trained $S_\theta(K_w^t)$; $S_\theta(K_m^t)$

1: Setting: $\{K_w^t, K_m^t, z^t\} \sim N(0, I_{ax \times bx \times c})$; $1 \leq t \leq T$

2: **for** $t = T_{tol}$ **do**

3: $K_w^t = K_w^{t+1} + \frac{\epsilon}{2} S_\theta(K_w) + \sqrt{\epsilon} F[z_1^t]$

4: $K_m^t = K_m^{t+1} + \frac{\epsilon}{2} S_\theta(K_m) + \sqrt{\epsilon} F[z_2^t]$

5: **end for**

6: Update $K_w^t(k)$ and $K_m^t(k)$

7: Combination: $K^t = \begin{cases} \mu_2 K_m^t \{(\mu_1(K_w^t))\}; & Serial \\ \lambda_1(K_w^t) + \lambda_2(K_m^t); & Parallel \end{cases}$

8: Data Consistency:

$$k(u) = \begin{cases} K^t(u); & if u \notin \Omega \\ \frac{[A^T f + \lambda K^t(u)]}{(1+\lambda)}; & if u \in \Omega \end{cases}$$

9: Traditional Operator:

$$\min_k \|Ak - y\|_2^2 \text{ s.t. } \text{rank}(L) = l, k = H^+(L)$$

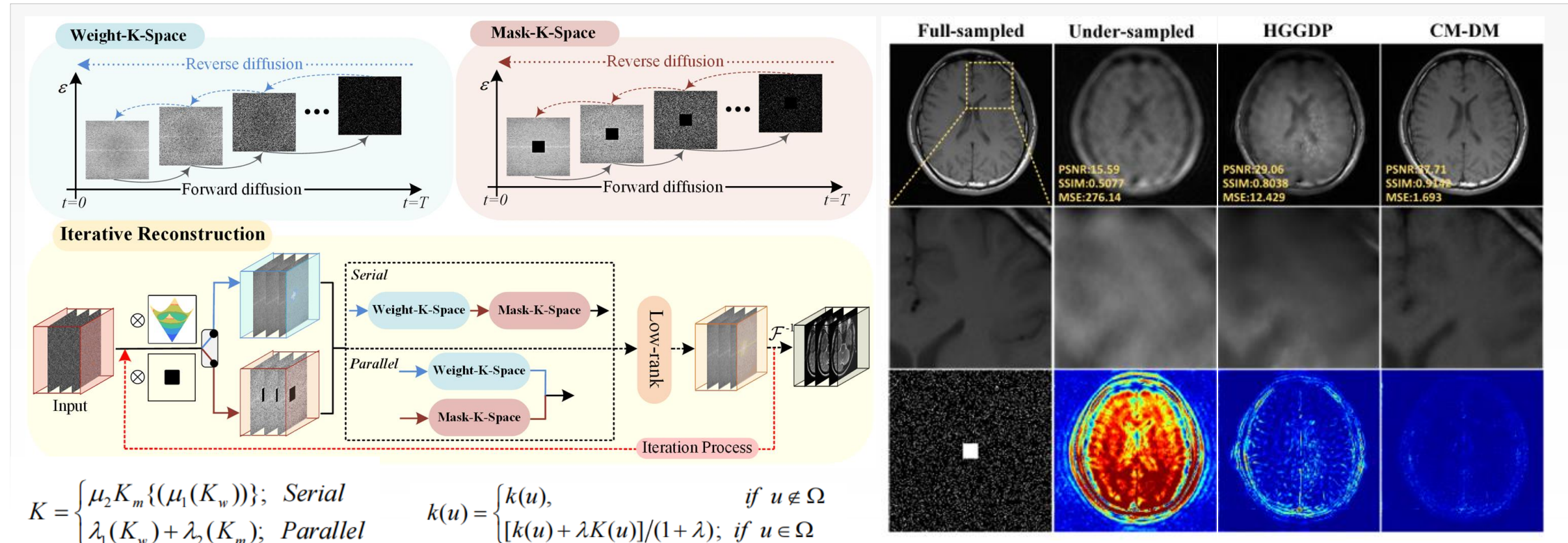
10: **return** k

以Mask作为引导加速收敛，进行差异化扩散建模与高频先验约束，提升观测域重建精度

研究内容

CM-DM

Correlated and Multi-frequency Diffusion Modeling for Highly Under-sampled MRI Reconstruction



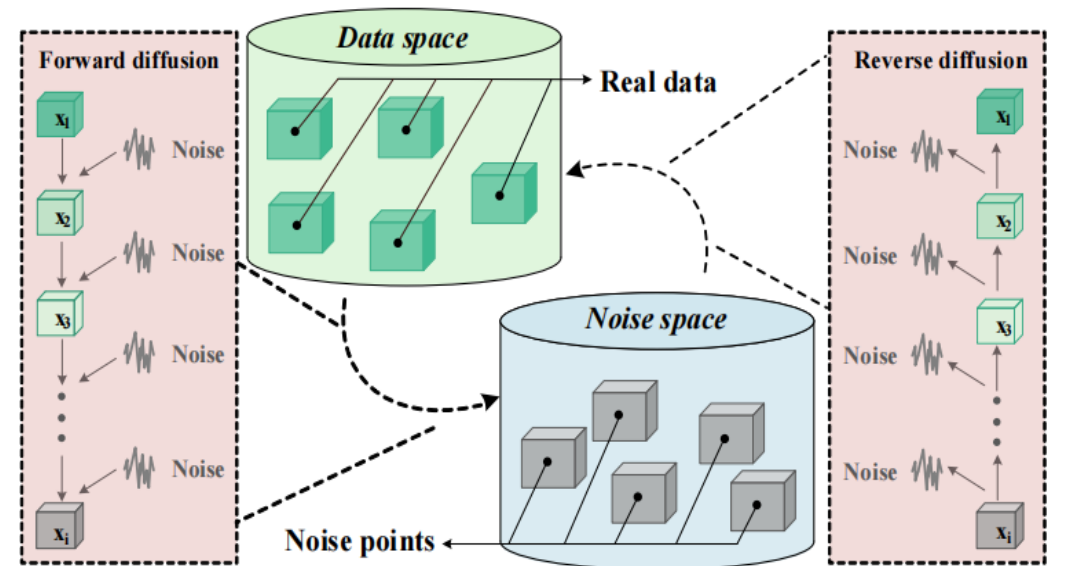
Y. Guan et al., IEEE Transactions on Medical Imaging, vol. 43, no. 10, pp. 3490–3502, Oct. 2024.

研究内容

Sub-DM Subspace Diffusion Model with Orthogonal Decomposition for MRI Reconstruction

基于K空间小波域多分布驱动的MRI重建

小波空间



数学模型

Subspace Diffusion :

$$g(t) = g(t)\mathbf{Q}_m \mathbf{Q}_m^T,$$

$$\mathbf{f}(k, t) = f(t)k + \sum_{m=1}^T \delta(t - t_m)(\mathbf{Q}_m \mathbf{Q}_m^T - \mathbf{I}_d)k,$$

Orthogonal Decomposition:

$$\begin{aligned} \{k^{LL}, k^{LH}, k^{HL}, k^{HH}\} &= Wk, \\ \langle k^i, k^j \rangle &= 0, \quad i \neq j \in \{LL, LH, HL, HH\}, \end{aligned}$$

面向 MRI子空间建模，通过将扩散过程限制在低维紧致子空间中，显著缓解收敛缓慢的问题

研究内容

Sub-DM Subspace Diffusion Model with Orthogonal Decomposition for MRI Reconstruction

利用正交分解将观测域映射至结构化子空间，使扩散过程在高噪声演化阶段保持有效信息，大幅降低迭代数量

$$\theta^* = \min_{\theta} \mathbb{E}_t \{ \lambda_t \mathbb{E}_{k(0)} \mathbb{E}_{k(t)|k(0)} [\| s_{\theta}(k(t), t) - \nabla_{k(t)} \log p_t(k(t)|k(0)) \|_2^2] \}.$$

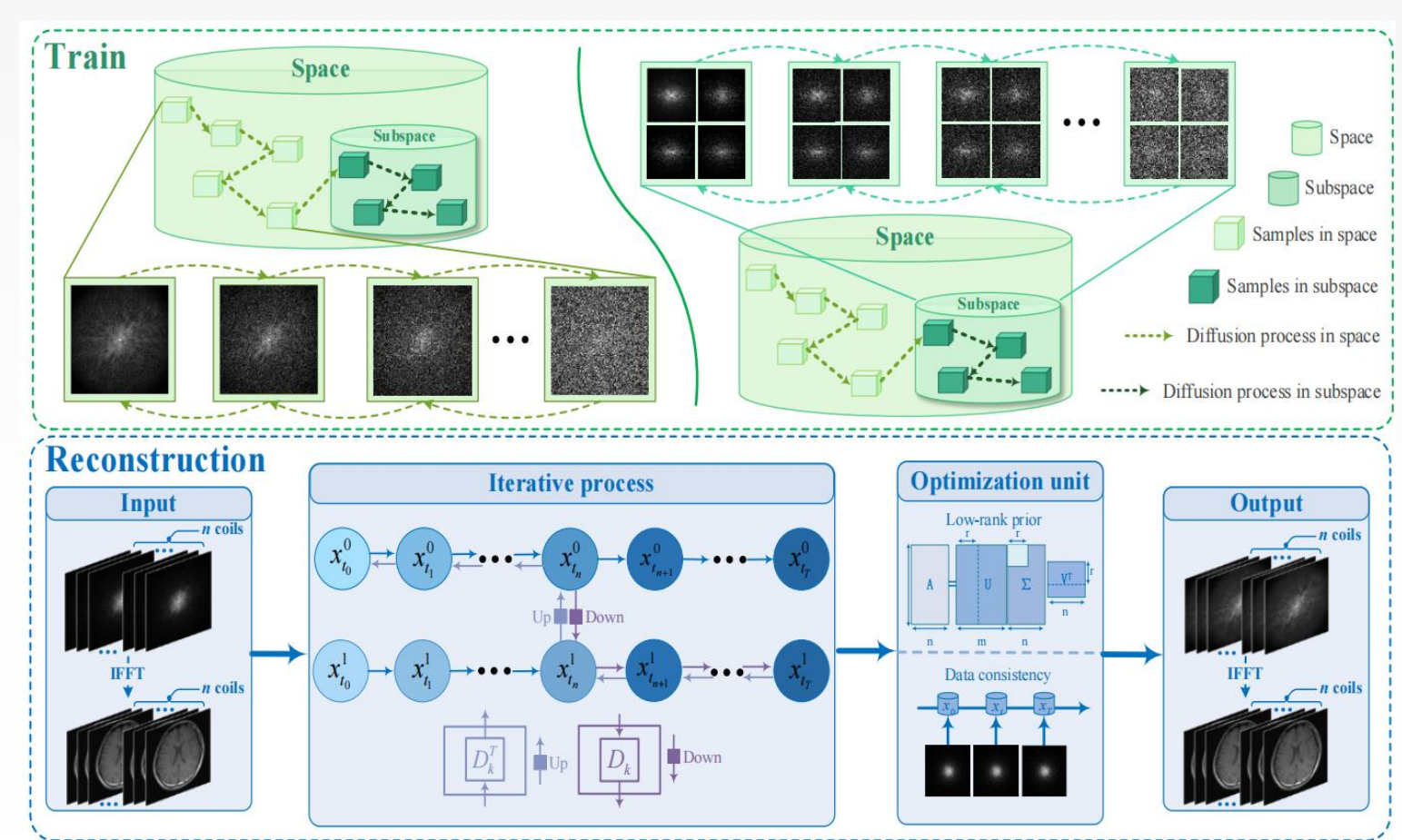
$$\theta_S^* = \min_{\theta_S} \mathbb{E}_t \{ \lambda_t \mathbb{E}_{\mathbb{K}(0)} \mathbb{E}_{\mathbb{K}(t)|\mathbb{K}(0)} [\| s_{\theta_S}(\mathbb{K}(t), t) - \nabla_{\mathbb{K}(t)} \log p_t(\mathbb{K}(t)|\mathbb{K}(0)) \|_2^2] \}.$$

$$k_{t-1} = k_t + (\sigma_t^2 - \sigma_{t-1}^2) s_{\theta}(k_t, t) + \sqrt{\sigma_t^2 - \sigma_{t-1}^2} Z,$$

$$k_{t-1} = k_{t-1} + \varepsilon_{t-1} s_{\theta}(k_{t-1}, t) + \sqrt{2\varepsilon_{t-1}} Z,$$

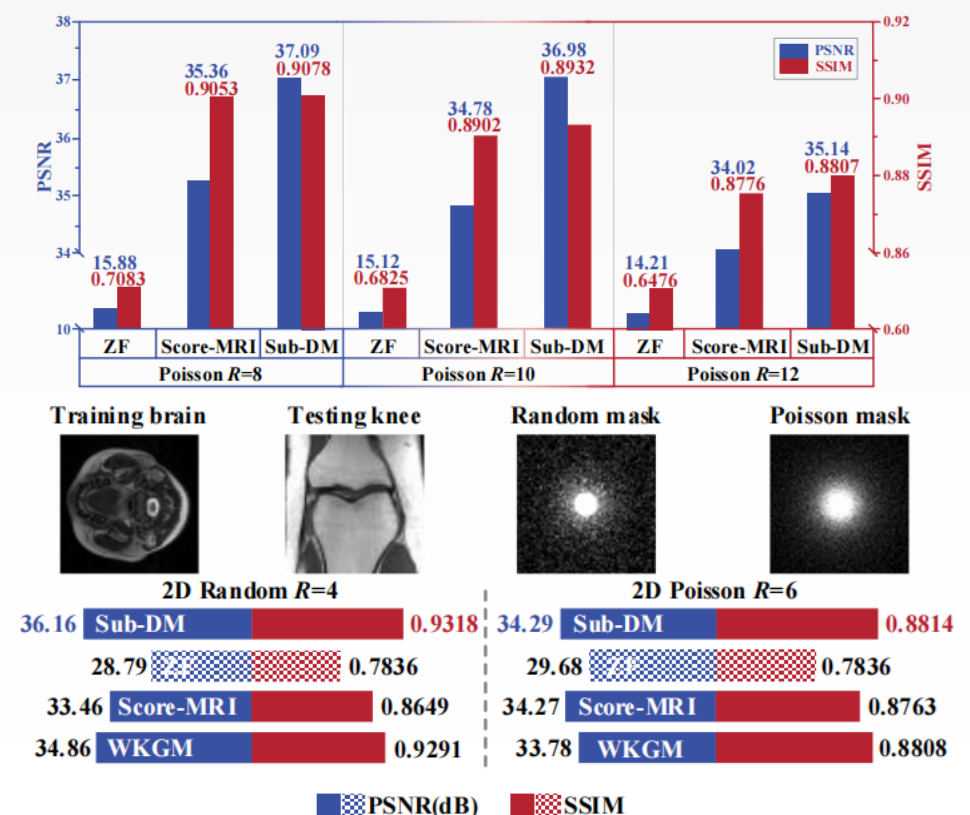
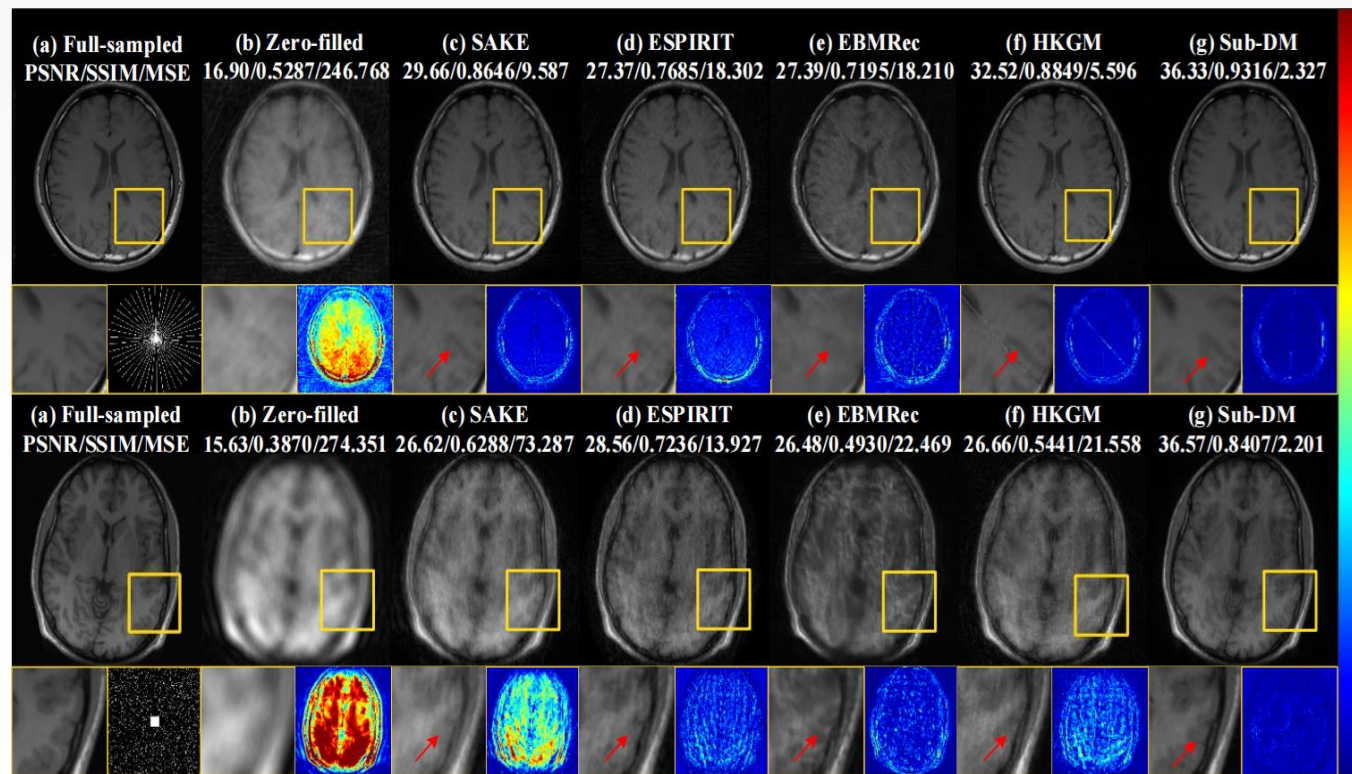
$$\mathbb{K}_{t-1} = \mathbb{K}_t + (\sigma_t^2 - \sigma_{t-1}^2) s_{\theta_S}(\mathbb{K}_t, t) + \sqrt{\sigma_t^2 - \sigma_{t-1}^2} Z.$$

$$\mathbb{K}_{t-1} = \mathbb{K}_{t-1} + \varepsilon_{t-1} s_{\theta_S}(\mathbb{K}_{t-1}, t) + \sqrt{2\varepsilon_{t-1}} Z.$$



研究内容

Sub-DM Subspace Diffusion Model with Orthogonal Decomposition for MRI Reconstruction



Y. Guan, Q. Cai, W. Li, Q. Fan, D. Liang, and Q. Liu, IEEE Transactions on Computational Imaging, vol. 12, pp. 309–320, 2026.

研究内容

GMSD

Generative modeling in sinogram domain for sparse-view CT reconstruction

基于高维先验的无监督CT稀疏角重建

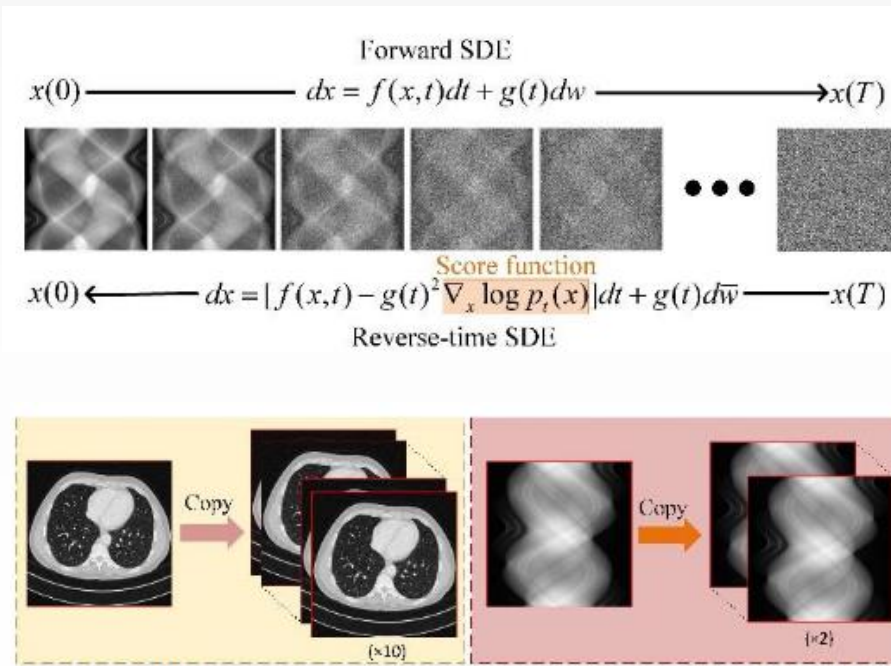
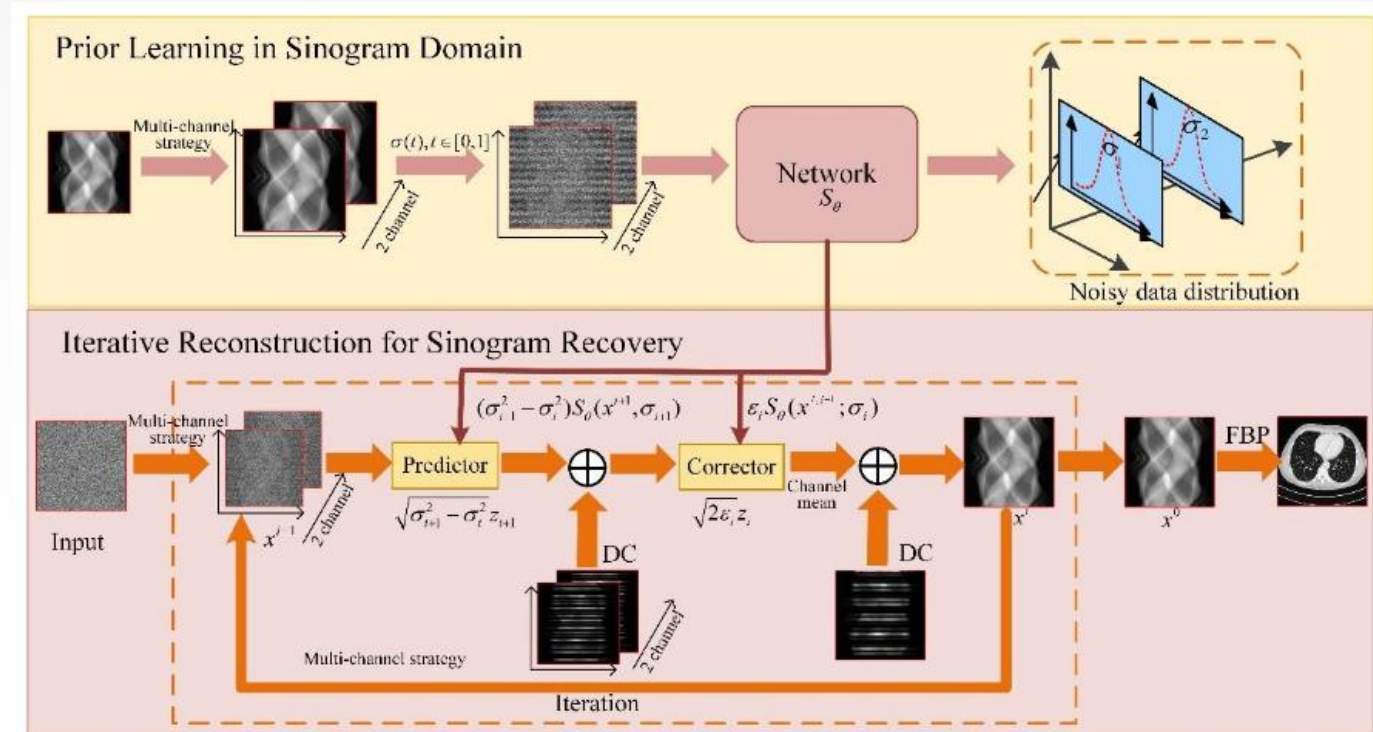


Fig. 3. Multi-channel strategy in different methods. (a) EASEL (b) GMSD.



多通道正弦图建模策略以刻画高维投影结构，实现无监督生成式重建

研究内容

GMSD

Generative modeling in sinogram domain for sparse-view CT reconstruction

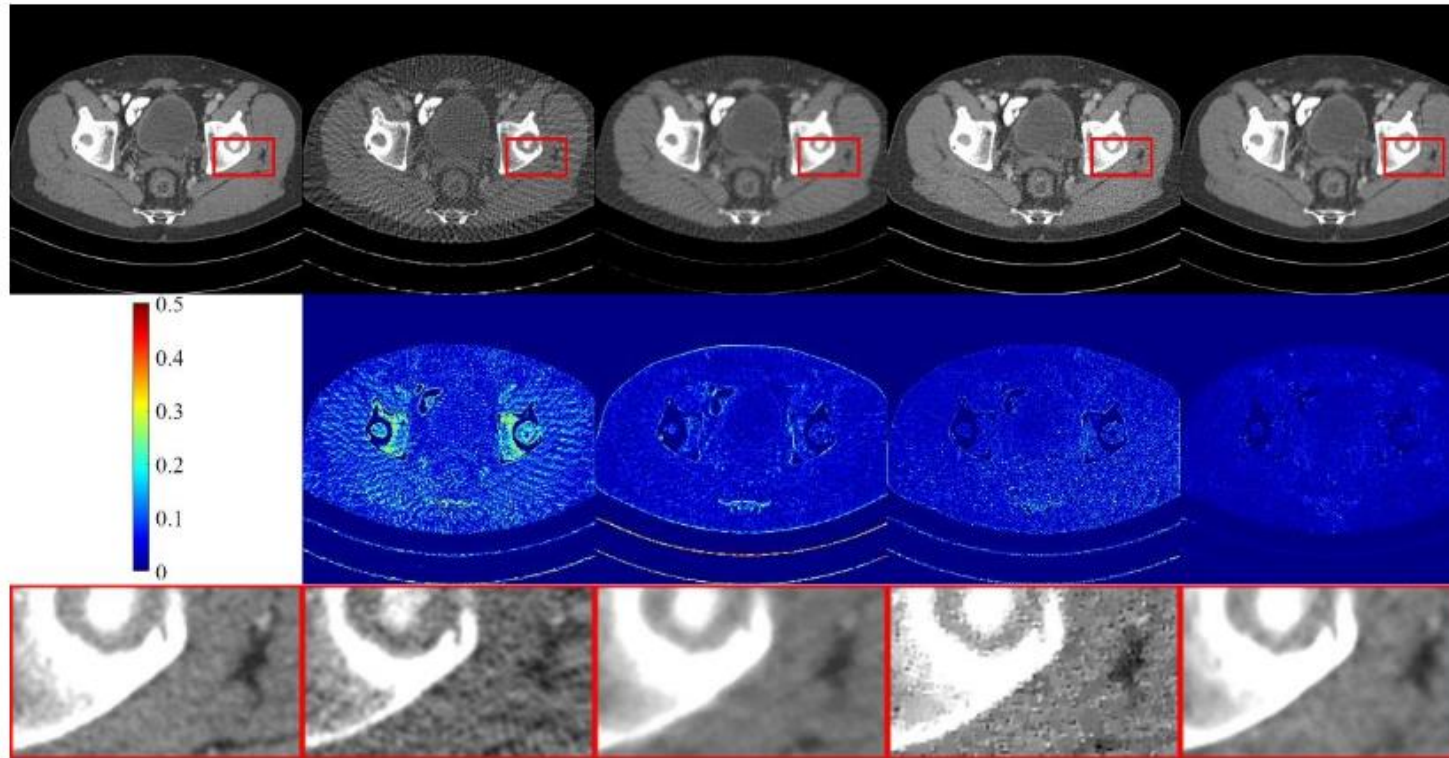
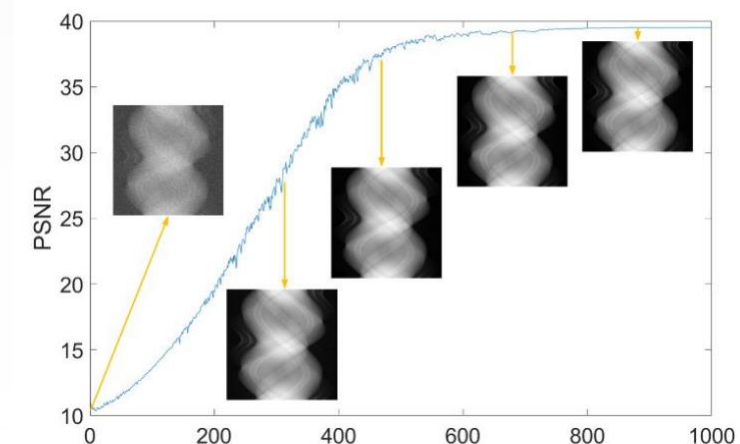


TABLE IV
THE IMPACT OF CHANNEL NUMBER ON GMSD RECONSTRUCTION.

Channel	Index	60	90	120	180
1-ch	PSNR	35.26	37.71	39.37	41.66
	SSIM	0.9621	0.9753	0.9818	0.9869
	MSE	0.00032	0.00019	0.00012	0.00008
2-ch	PSNR	35.74	38.93	39.90	42.82
	SSIM	0.9607	0.9804	0.9855	0.9909
	MSE	0.00030	0.00014	0.00010	0.00006



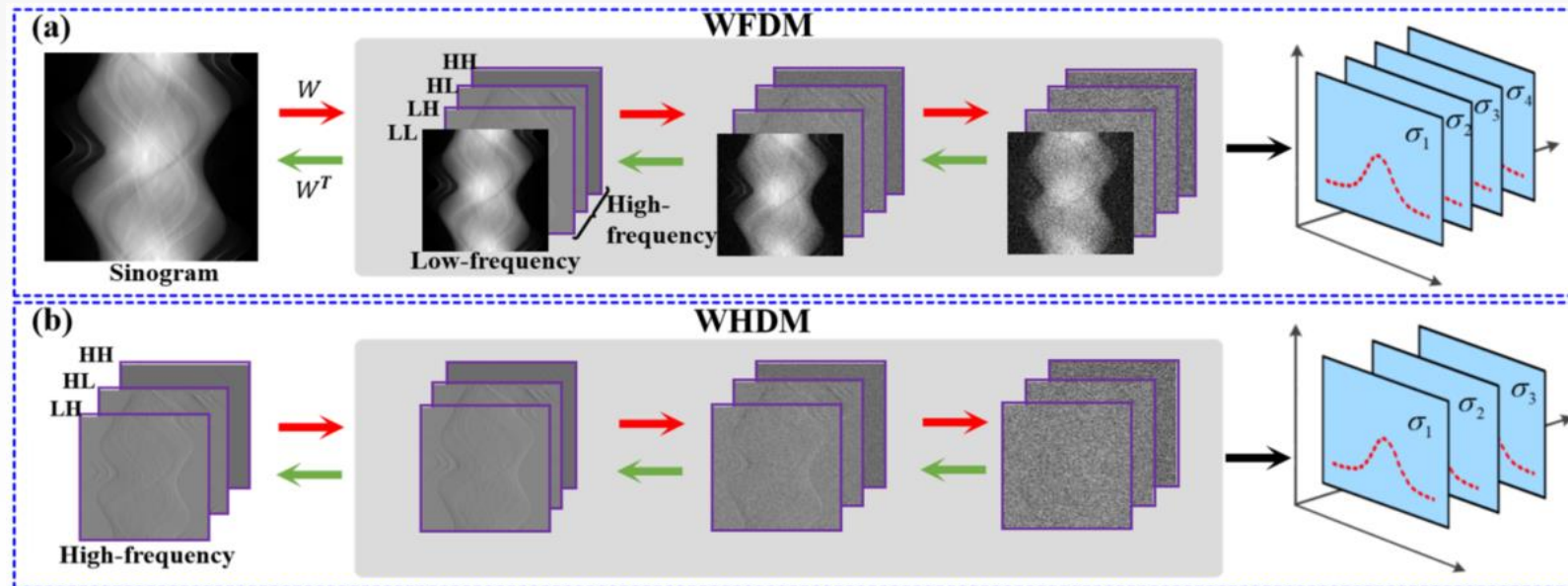
研究内容

SWORD

Stage-by-stage Wavelet Optimization Refinement Diffusion Model for Sparse-View CT Reconstruction

小波分解驱动CT多分布构造

迭代算法



$$\theta_1^* = \underset{\theta_1}{\operatorname{argmin}} \mathbb{E}_t \left\{ \lambda(t) \mathbb{E}_{X_1(0)} \mathbb{E}_{X_1(t)|X_1(0)} \left[\| s_{\theta_1}(X_1(t), t) - \nabla_{X_1(t)} \log p_t(X_1(t)|X_1(0)) \|_2^2 \right] \right\}$$

$$\{X_1^*, X_2^*\} = \underset{\{X_1, X_2\}}{\operatorname{argmin}} \left[\|X_1 - WP(\Lambda)y\|_2^2 + \lambda_1 \|X_2 - E(X_1)\|_2^2 + \lambda_2 R_1(X_1) + \lambda_3 R_2(X_2) \right]$$

低频生成—高频精修—域变换

Algorithm 1 SWORD

Training Process

- 1: Generating projection x ;
- 2: Wavelet transform (WT):
 $W(x) = \{a_{LL}(x), d_{LH}(x), d_{HL}(x), d_{HH}(x)\}$;
- 3: Training datasets construction:
 $X_1 = \{a_{LL}(x), d_{LH}(x), d_{HL}(x), d_{HH}(x)\}$;
 $X_2 = \{d_{LH}(x), d_{HL}(x), d_{HH}(x)\}$;
- 4: Training with Eq. (9);
- 5: Output: $s_{\theta_1}(X_1, t)$ and $s_{\theta_2}(X_2, t)$.

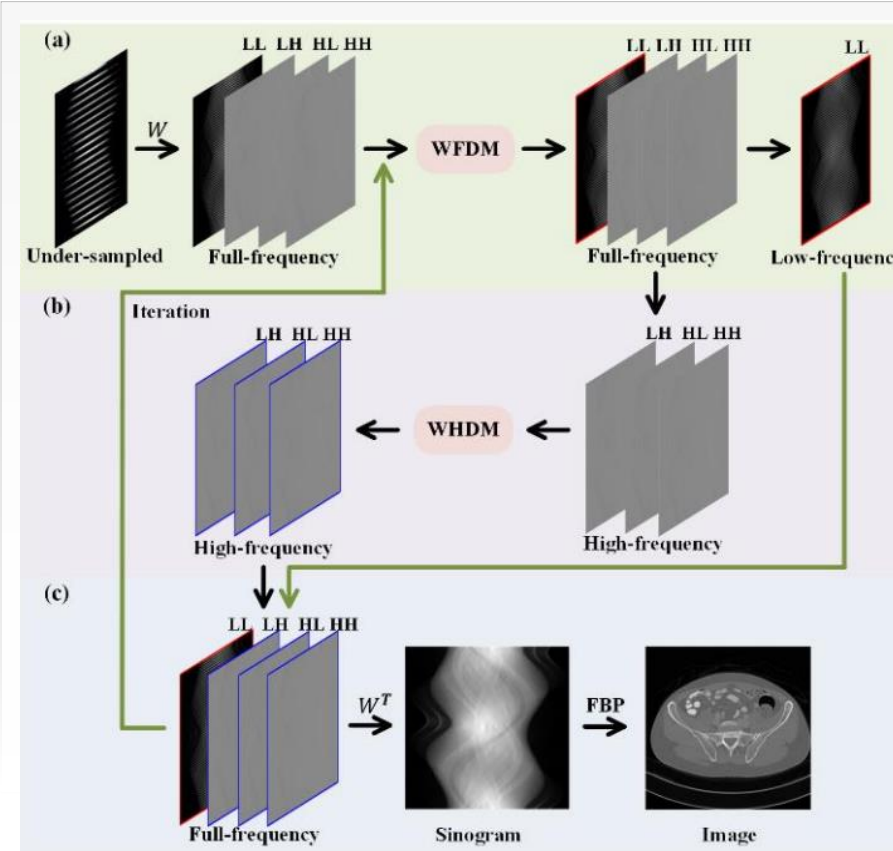
Inference Process

- Setting:** $s_{\theta_1}, s_{\theta_2}, T, \sigma, \varepsilon$
- 1: $X_1^T \sim N(0, \sigma_{max}^2), X_2^T \sim N(0, \sigma_{max}^2)$
 - 2: For $i = T - 1$ to 0 do
 - 3: Update $X_1^i \leftarrow Predictor(X_1^{i+1}, \sigma_i, \sigma_{i+1})$;
 - 4: Update X_1^i by data consistency with Eq. (12a);
 - 5: Update $X_1^i \leftarrow Corrector(X_1^i, \sigma_i, \varepsilon_i)$;
 - 6: Update X_1^i by data consistency with Eq. (12a);
 - 7: Repeat steps 3-6 by replacing X_1 with X_2 ;
 - 8: End for
 - 9: Achieving the reconstructed image by Eq. (16);
 - 10: Return I .

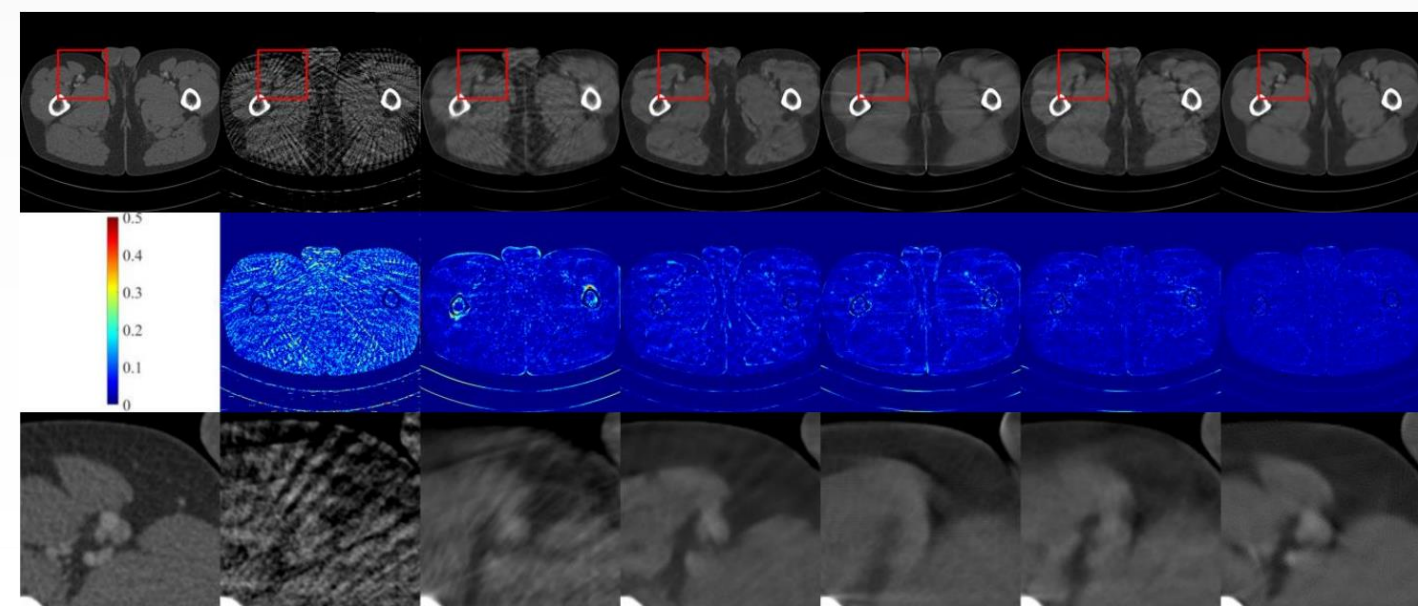
研究内容

SWORD

Stage-by-stage Wavelet Optimization Refinement Diffusion Model for Sparse-View CT Reconstruction



Views	FBP	U-Net	FBPCovNet	patch-based DDPM	GMSD	SWORD
60	23.18/0.5950/4.88	28.83/0.9365/1.56	35.63/0.9659/0.28	32.04/0.9336/0.68	34.31/0.9580/0.41	38.49/0.9778/0.15
90	26.20/0.7013/2.45	30.09/0.9472/1.17	37.11/0.9758/0.25	35.15/0.9634/0.35	37.25/0.9739/0.20	41.27/0.9862/0.08
120	28.30/0.7865/1.52	35.58/0.9765/0.34	39.45/0.9828/0.15	37.90/0.9759/0.17	39.41/0.9812/0.12	42.49/0.9895/0.06
180	31.69/0.8820/0.70	38.37/0.9853/0.19	42.23/0.9881/0.07	40.95/0.9845/0.09	41.44/0.9876/0.08	45.08/0.9941/0.03



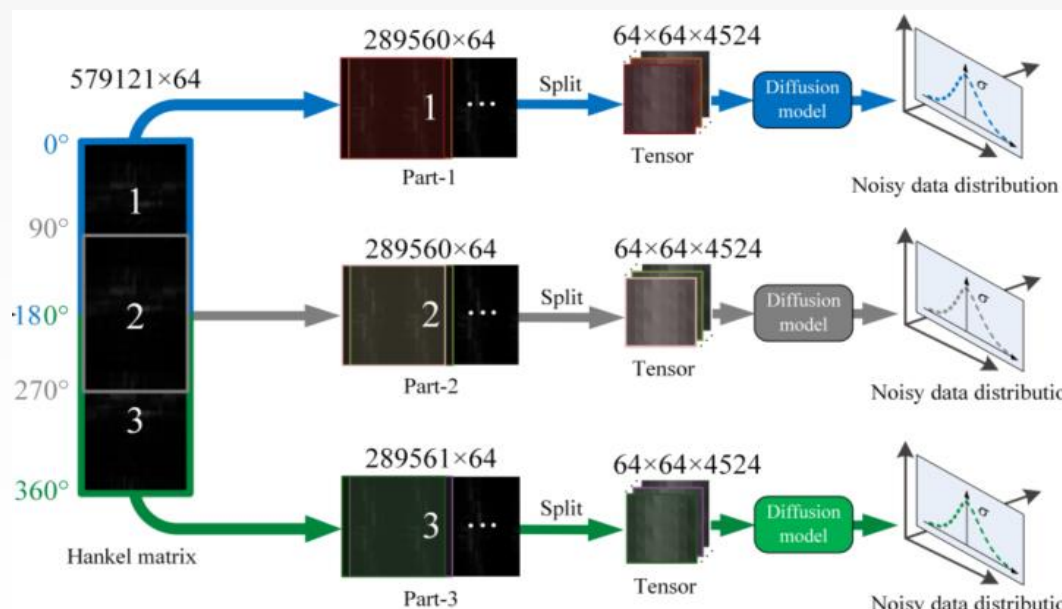
Xu, K., Lu, S., Huang, B., Wu, W., and Liu, Q., IEEE Transactions on Medical Imaging, vol. 43, no. 10, pp. 3412–3424, Oct. 2024.

研究内容

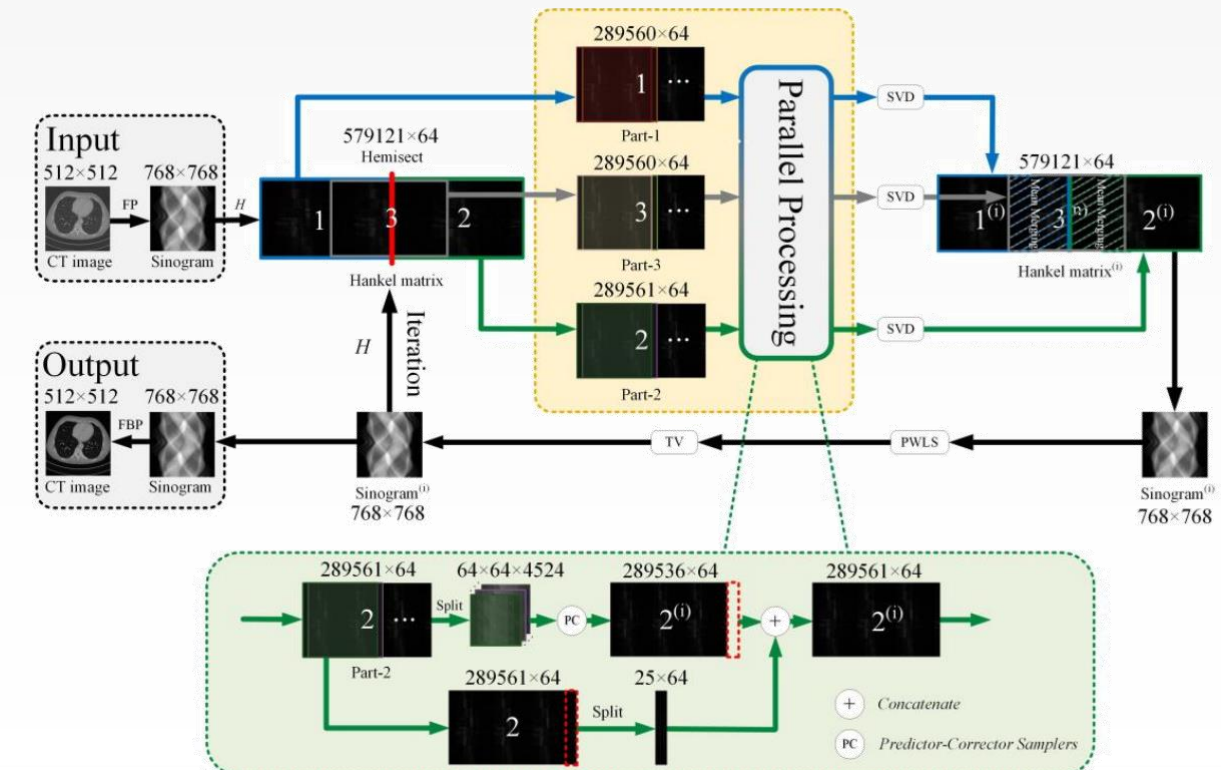
RAP

Low-rank Angular Prior Guided Multi-diffusion Model for Few-shot Low-dose CT Reconstruction

Hankel域多分布驱动的低剂量CT图像重建



$$\theta^* = \arg \min_{\theta} \mathbb{E}_t \{ \lambda(t) \mathbb{E}_{x(0)} \mathbb{E}_{x(t)|x(0)} [\| s_\theta(x(t), t) - \nabla_{x(t)} \log p_t(x(t) | x(0)) \|_2^2] \}$$



结合随机微分方程求解器与数据一致性约束，逐步优化投影数据

研究内容

RAP

Low-rank Angular Prior Guided Multi-diffusion Model for Few-shot Low-dose CT Reconstruction

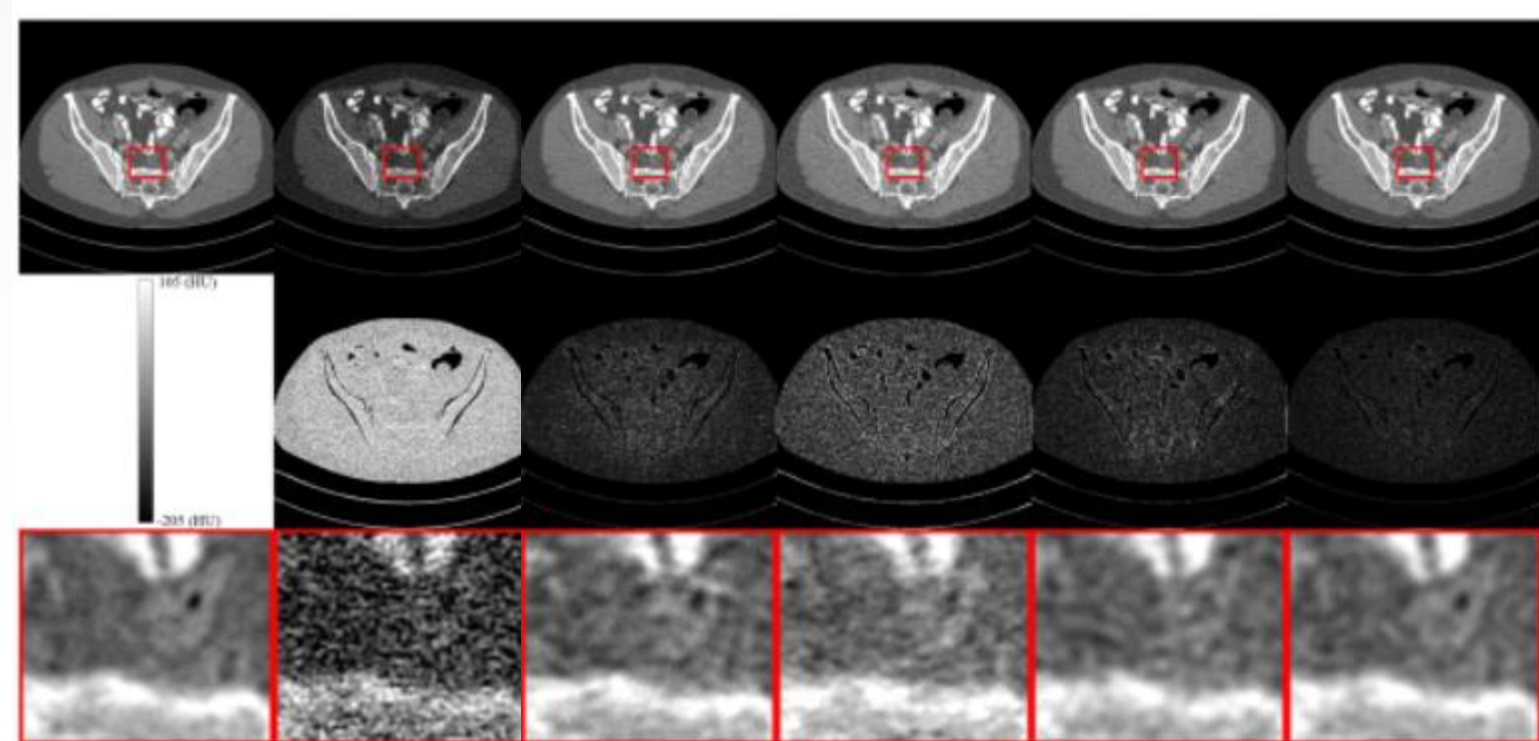
迭代算法

Iterative Reconstruction Stage

Setting: $s_\theta, N, M, \sigma, \varepsilon$

- 1: Initial data $x = F(I)$ (FP)
- 2: $x^N \sim \mathcal{N}(0, \sigma_{\max}^2 I)$
- 3: For $i = N-1$ to 0 do (Outer loop)
- 4: $x^i \leftarrow Predictor(x^{i+1}, \sigma_i, \sigma_{i+1}, s_\theta)$
- 5: $[H_1^i, H_2^i, H_3^i] = H_p^i \leftarrow H(x^i)$ (HT)
- 6: H_1^i, H_2^i, H_3^i via Eq. (17)
- 7: $[U \Delta V^T] = svd[H_1^i, H_2^i, H_3^i]^T$ (SVD)
- 8: $H_{[k]}^i = U_{[k]} \Delta_{[k]} V_{[k]}^T$ (hard-THR)
- 9: $x^i \leftarrow H^+(H_{[k]}^i)$ (IHT)
- 10: $x^i = \frac{W(y - x^{i+1}) + \mu R'(x^{i+1})}{W + \mu}$ (PWLS)
- 11: $x^i = TV(x^i)$ (TV)
- 12: For $j = 1$ to M do (Inner loop)
- 13: $x^{i,j} \leftarrow Corrector(x^{i,j-1}, \sigma_i, \varepsilon_i, s_\theta)$
- 14: Repeat from step 5 to step 11
- 15: End for
- 16: End for
- 17: Final image $\tilde{I} = F^{-1}(x)$ (FBP)
- 18: Return \tilde{I}

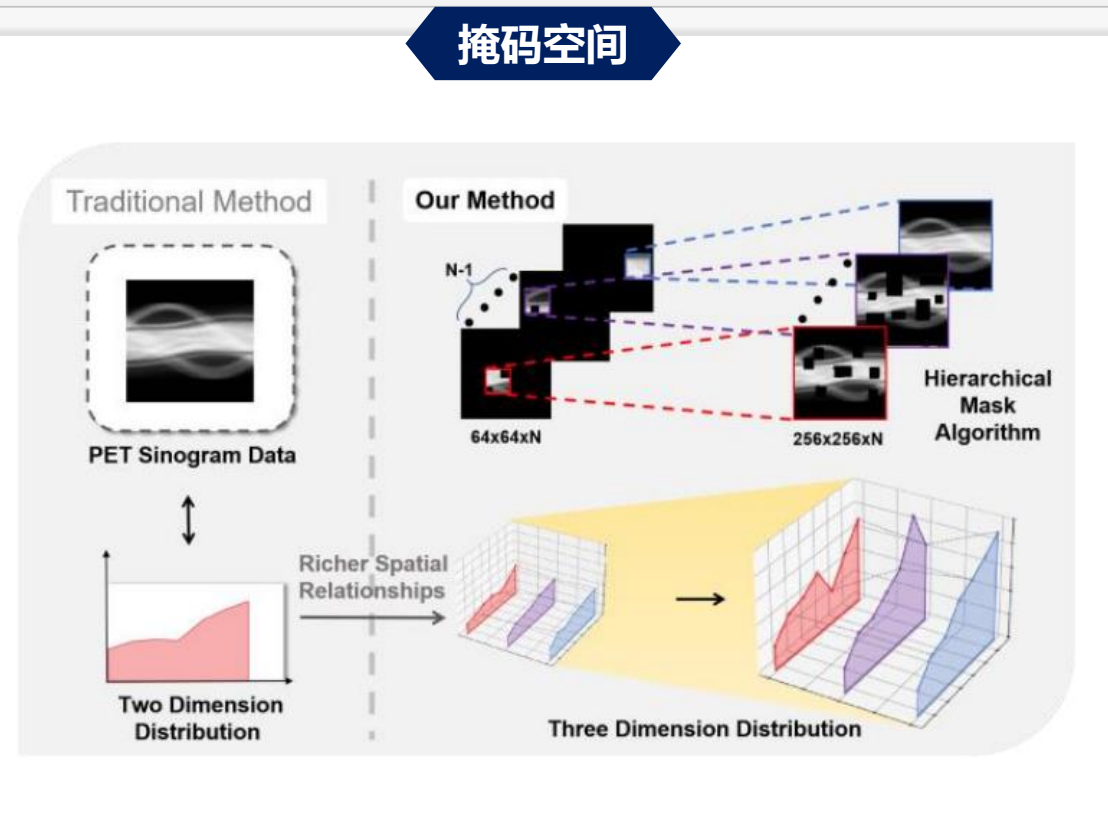
实验结果



研究内容

DREAM Diffusion Transformer Meets Random Masks: An Advanced PET Reconstruction Framework

基于随机掩码的多分布低剂量PET重建



模型算法

Masks :

$$I'(x, y) = I(x, y) \odot M(x, y)$$

Algorithm :

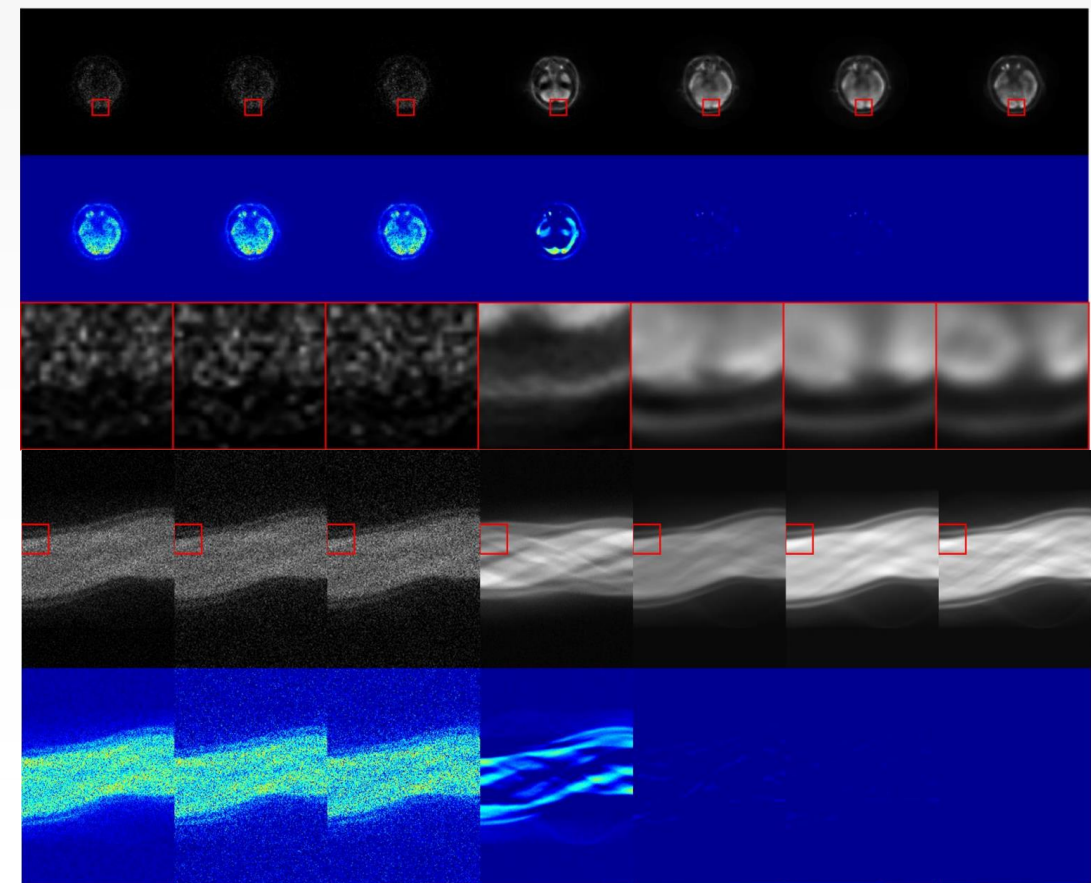
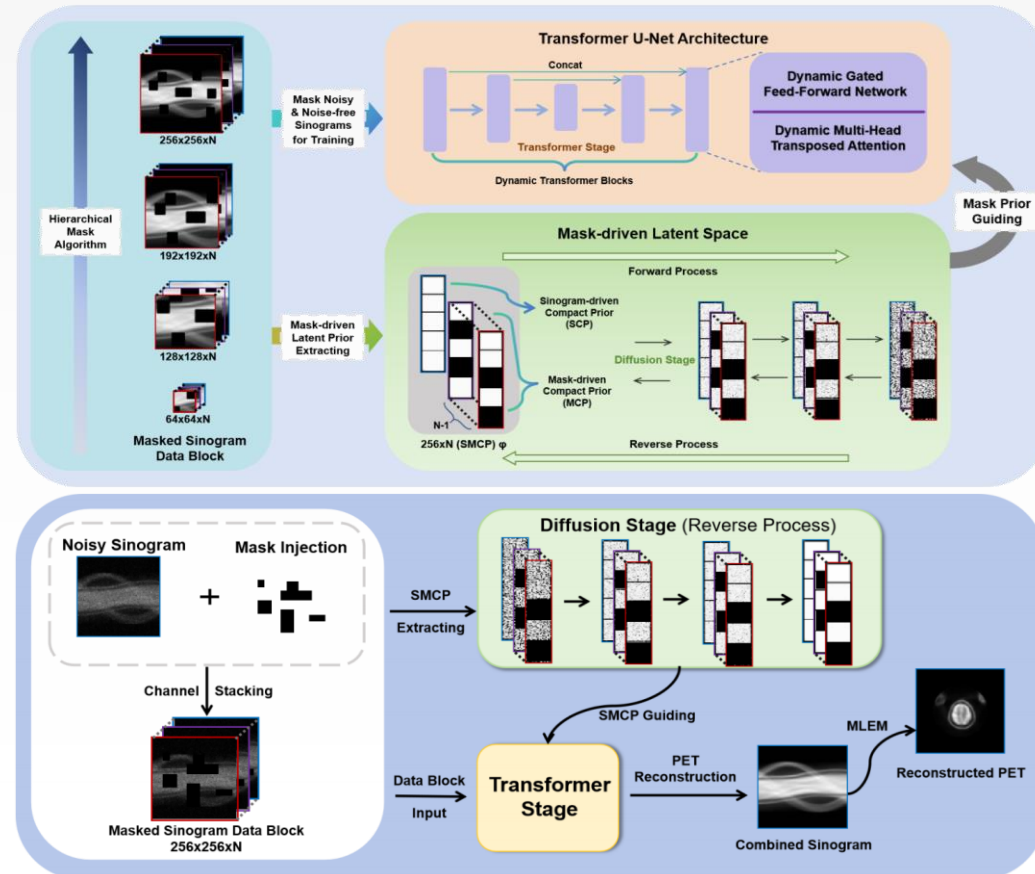
Require: $S^0, S_i^0, \lambda^0, \omega_i, \rho, \hat{\phi}, M, \mu$

- 1: **Initialization:** S'^0 , and λ^0
- 2: **For** $i = 0$ to convergence:
- 3: **Update** S'^{j+1} via Eq. (21)
- 4: **Update** λ^{j+1} via Eq. (22)
- 5: **End for**
- 6: **Final Reconstruction:** $I' = MLEM(S')$
- 7: **Return** I'

在正弦图域与潜空间同时融合掩膜建模，通过高维堆叠增强对空间相关性的建模能力

研究内容

DREAM Diffusion Transformer Meets Random Masks: An Advanced PET Reconstruction Framework



B. Huang et al., arXiv preprint arXiv:2503.08339, 2025.

目录



目录

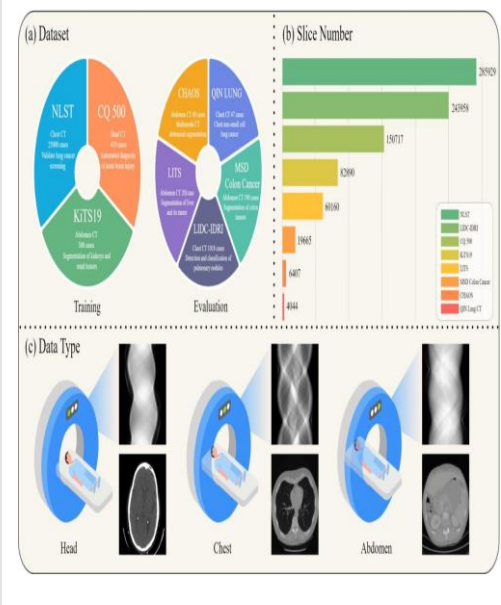
- 01 研究背景**
——从图像域走向原始观测域
- 02 核心突破**
——多分布表征的观测域成像建模
- 03 模型赋能**
——多任务驱动观测域智能生成

研究背景

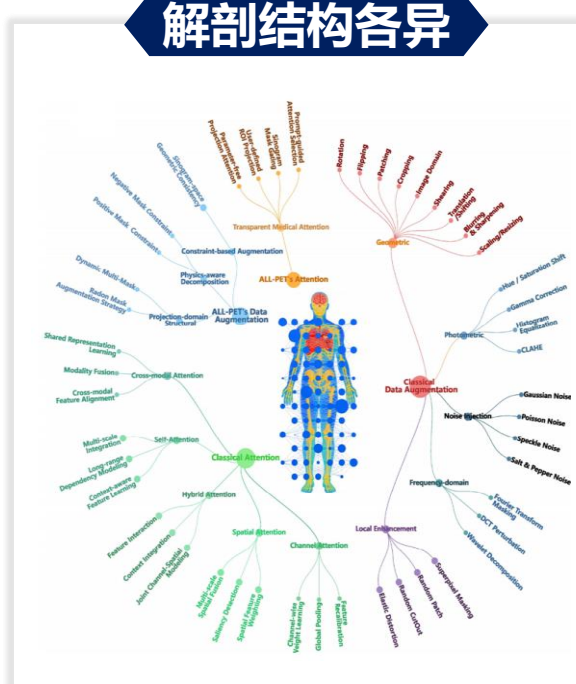
基础模型驱动 物理源头通解→下游任务统一

下游任务面临的问题

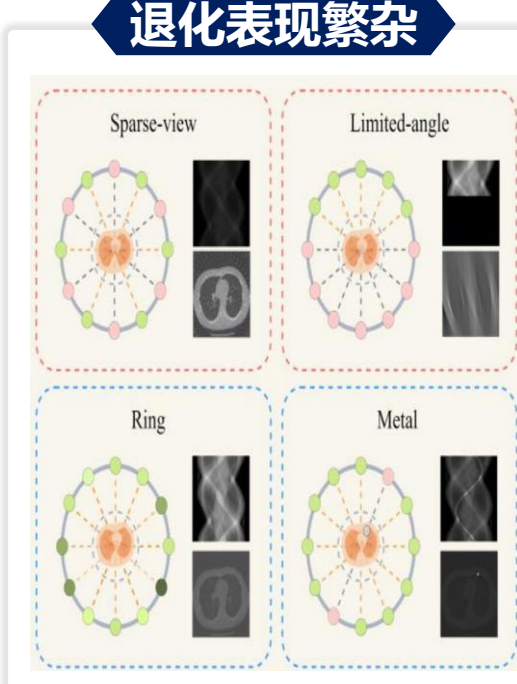
采集协议不同



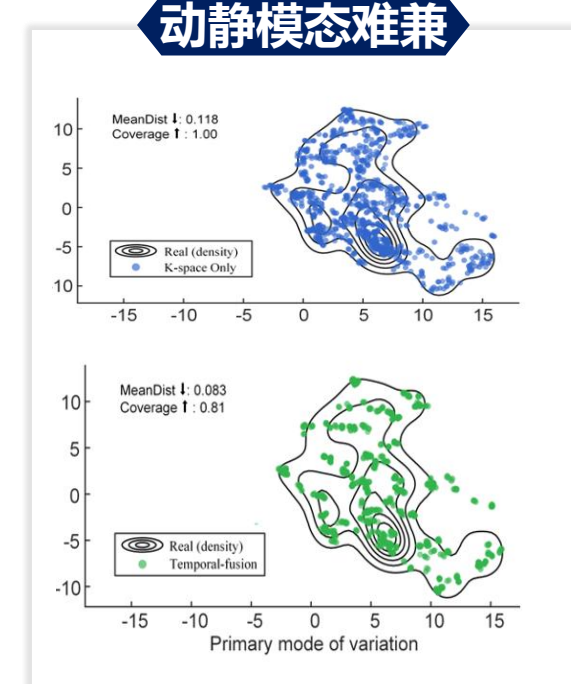
解剖结构各异



退化表现繁杂



动静模态难兼

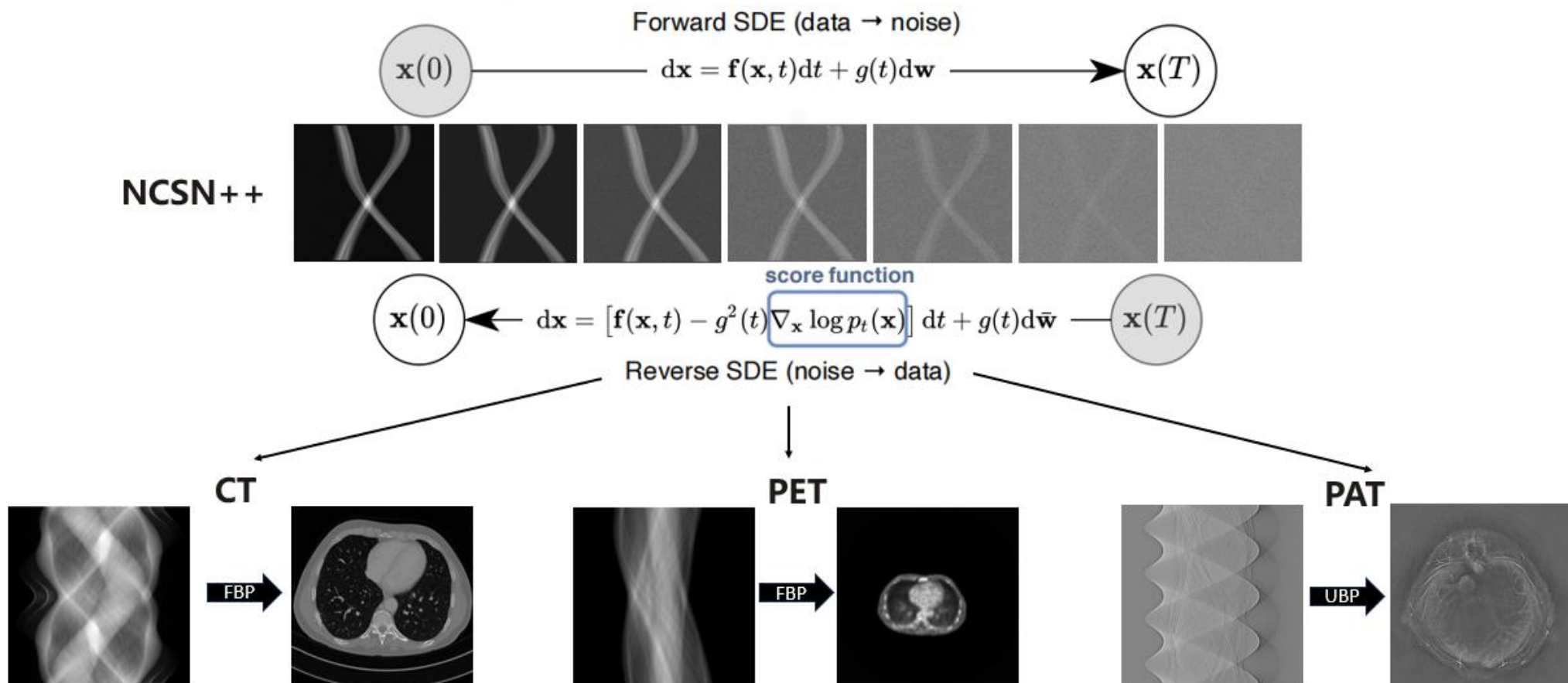


从“原始信号精准预测”走向“下游多任务统一生成”

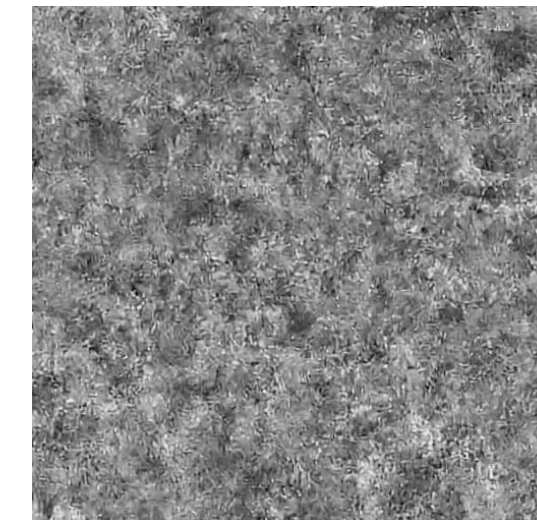
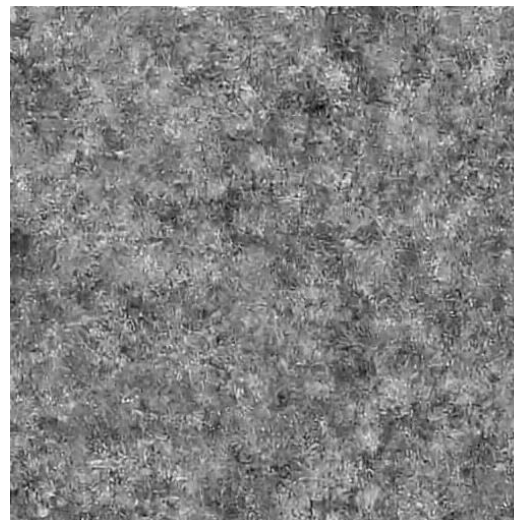
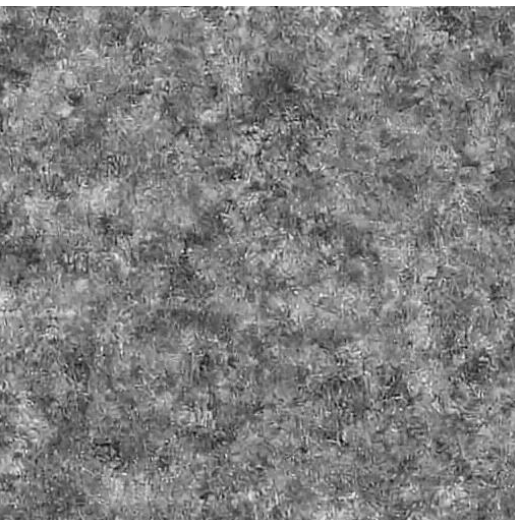
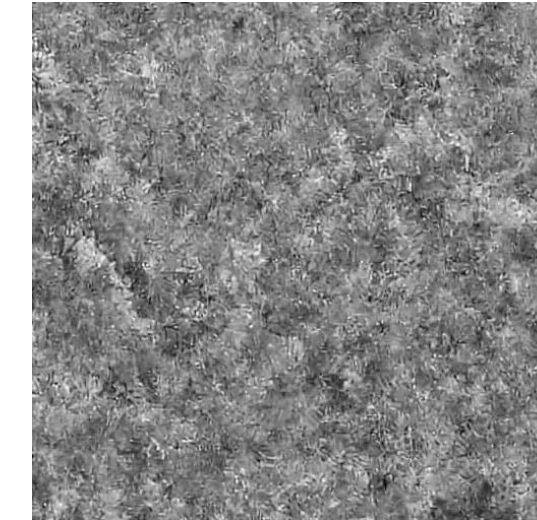
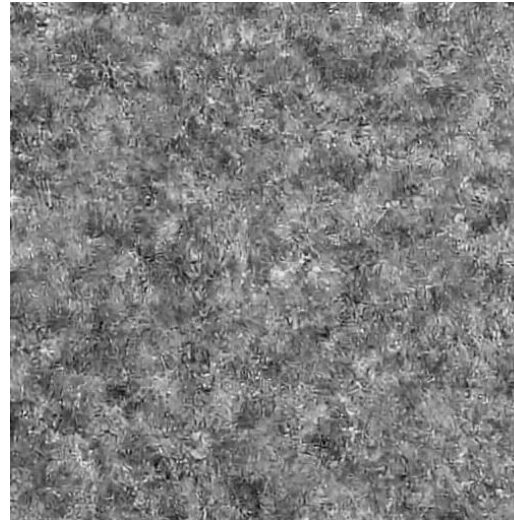
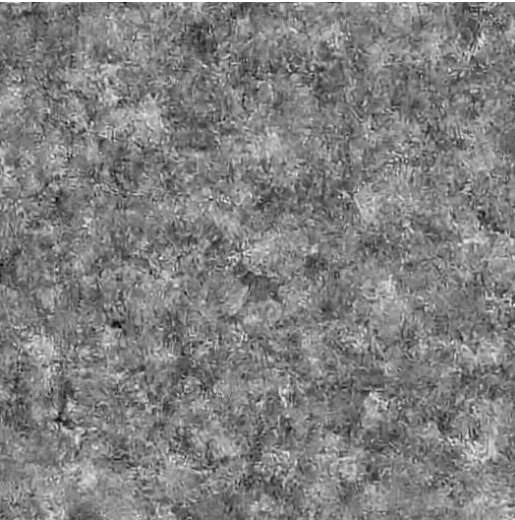
研究内容

基础模型驱动 原始域数据生成，为基础模型训练提供支持

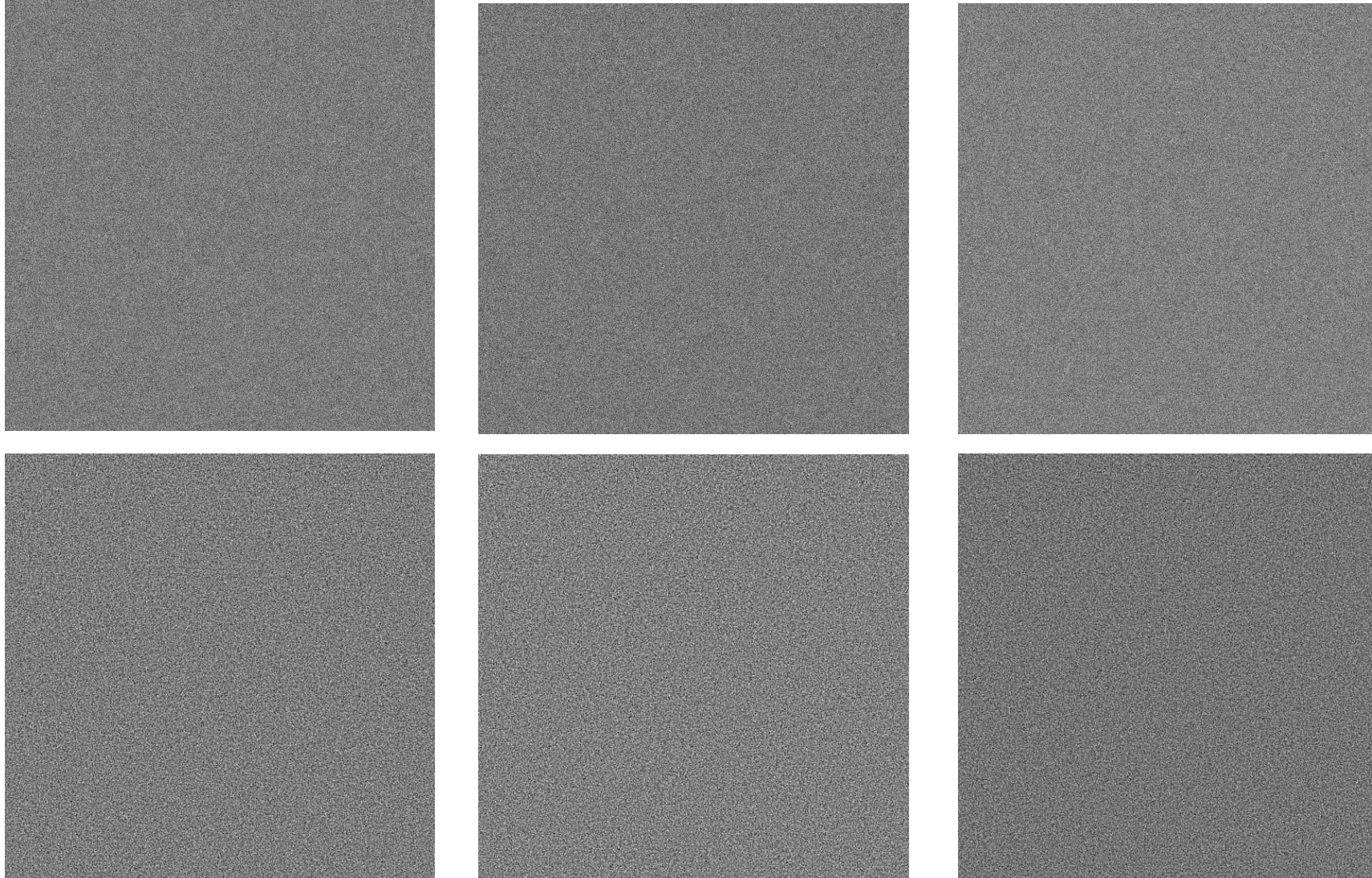
Raw data generation in Medical Imaging



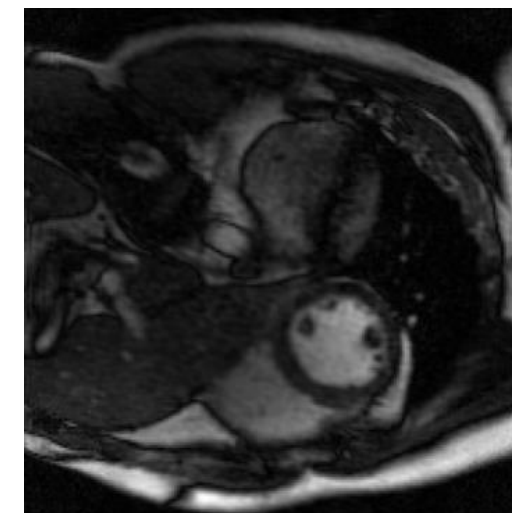
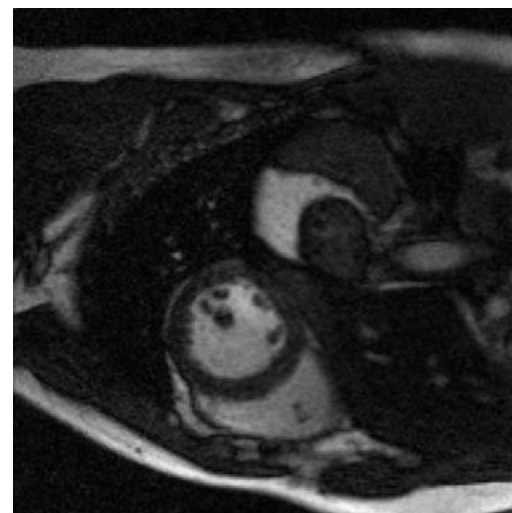
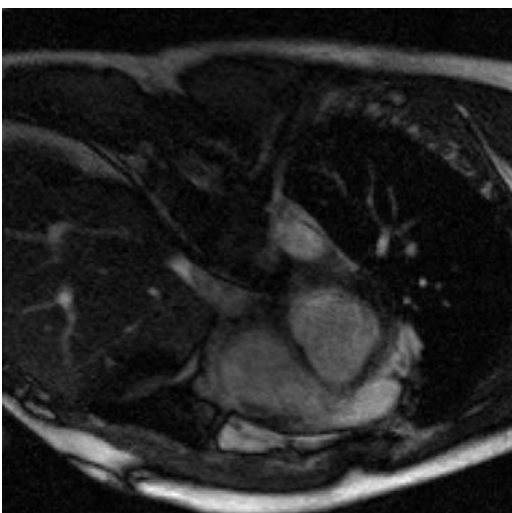
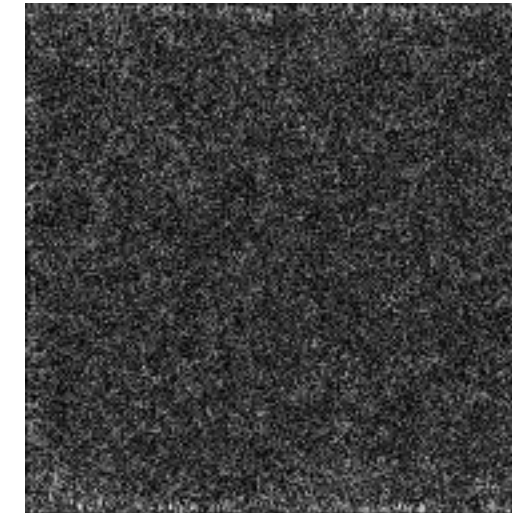
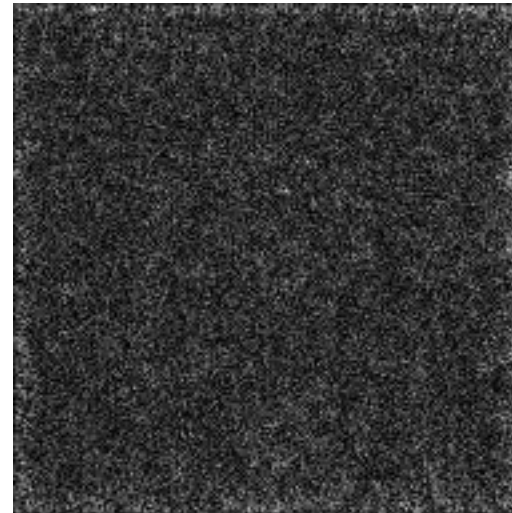
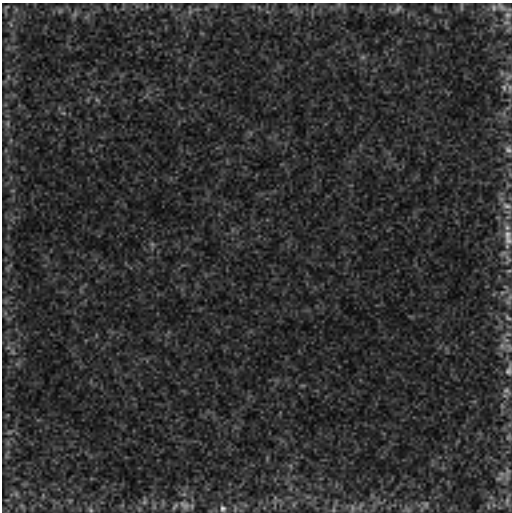
研究内容



研究内容



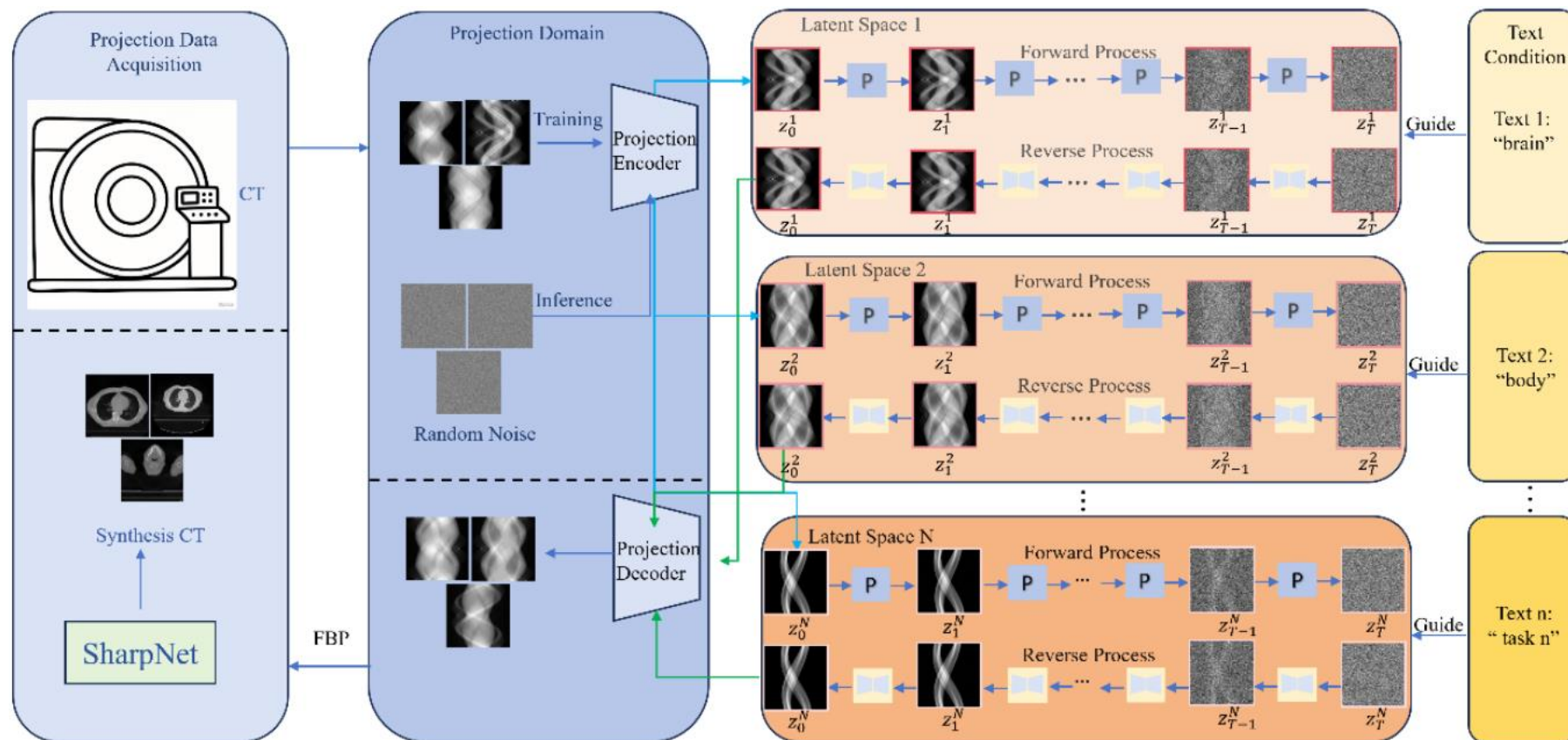
研究内容



PRO

PRO: Projection Domain Synthesis for CT Imaging

CT原始数据域数据生成模型

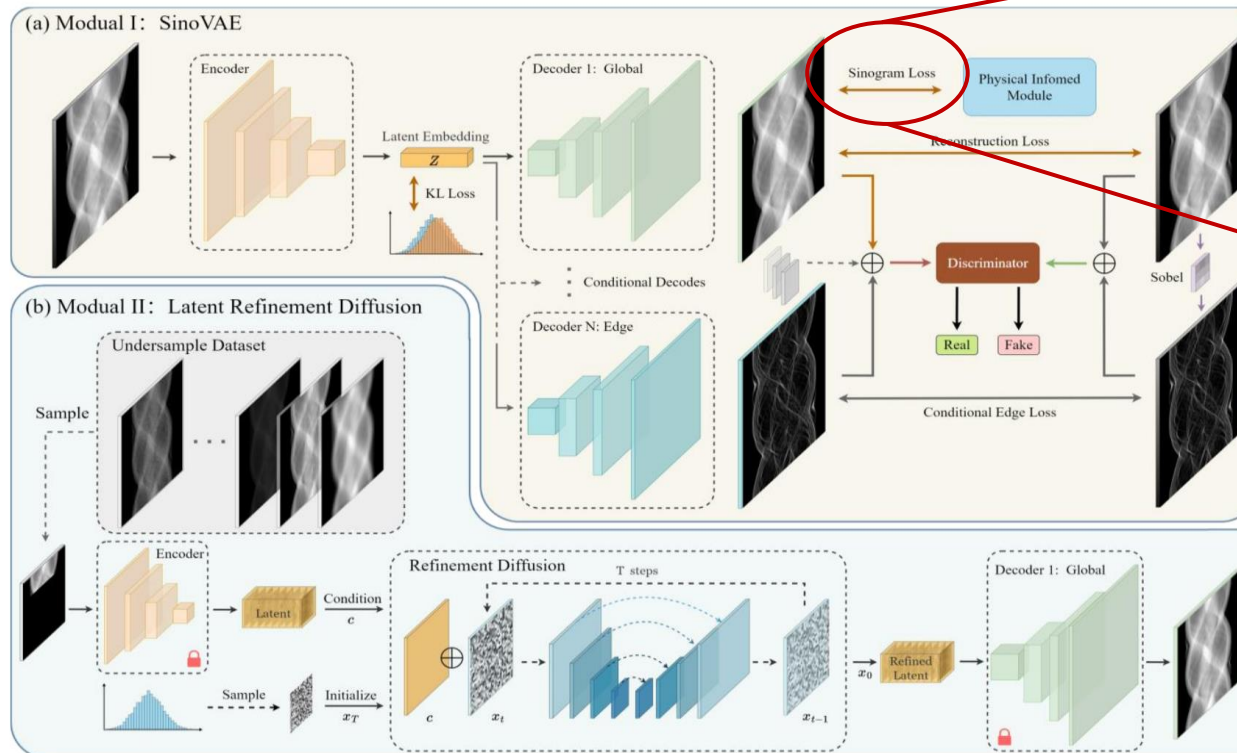


研究内容

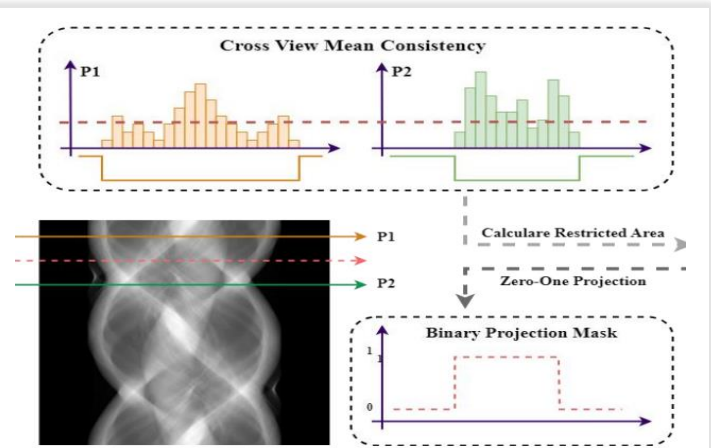
UniSino

UniSino: Physics-Driven Foundational Model for Universal CT Sinogram Standardization

物理驱动的CT正弦图标准化基础模型



物理引导的
SinoLoss



适用全种类伪影去除

Low-dose	$x_{LD}(s, \theta) = \ln \left[\frac{I_0}{Poisson(I_0 \exp(-x_0))} \right]$	Metal	$x_{ME}(s, \theta) = x_0 * (1 - P(\text{Mask}(f))) + C * P(\text{Mask}(f))$
Spares-view	$x_{SV}(s, \theta) = \text{Mask}_{\text{views}}(x_0)$	Geometry	$x_{GE}(s, \theta) = x_0(s + \Delta(\theta), \theta)$
Limited-angle	$x_{LA}(s, \theta) = W(\theta_1, \theta_2) * x_0$	Ring	$x_{RI}(s, \theta) = x_0(s, \theta) + a(s) * \text{Mask}(s)$
Truncate	$x_{TR}(s, \theta) = \begin{cases} x_0(s, \theta), & s \in [s_1, s_2] \\ 0, & \text{otherwise} \end{cases}$	Motion	$x_{MO}(s, \theta) = P(\mathcal{H}_\theta(f))$

研究内容

UniSino

UniSino: Physics-Driven Foundational Model for Universal CT Sinogram Standardization

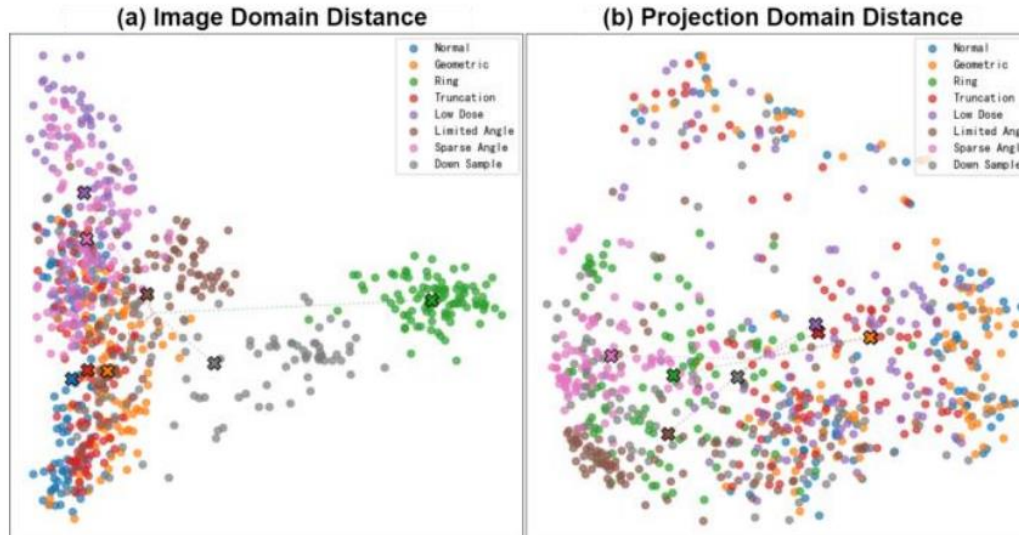


Table III
SINOGRAM COMPARISON ON NLST DATASET

Method	PSNR	SSIM	NRMSE
CycleGan	28.71	79.542	0.08253
ViT	32.96	74.856	0.01959
U-Net	41.53	91.625	0.01254
DDPM	43.56	94.411	0.00842
UniSino	46.19	96.731	0.00331

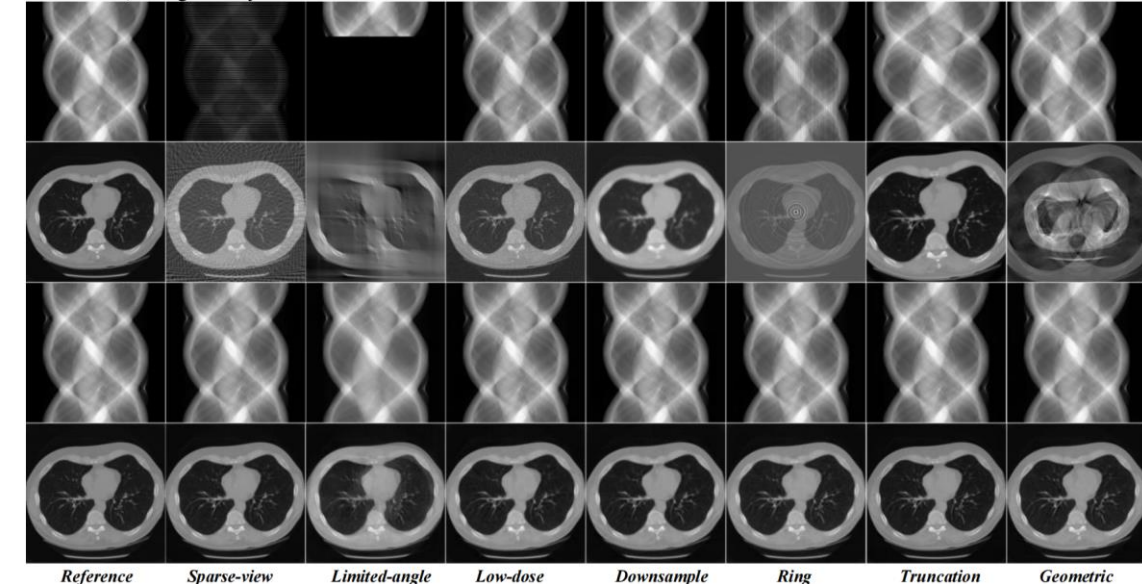


Table II
SINOGRAM STANDARDIZATION COMPARISON OF PSNR/SSIM/NRMSE

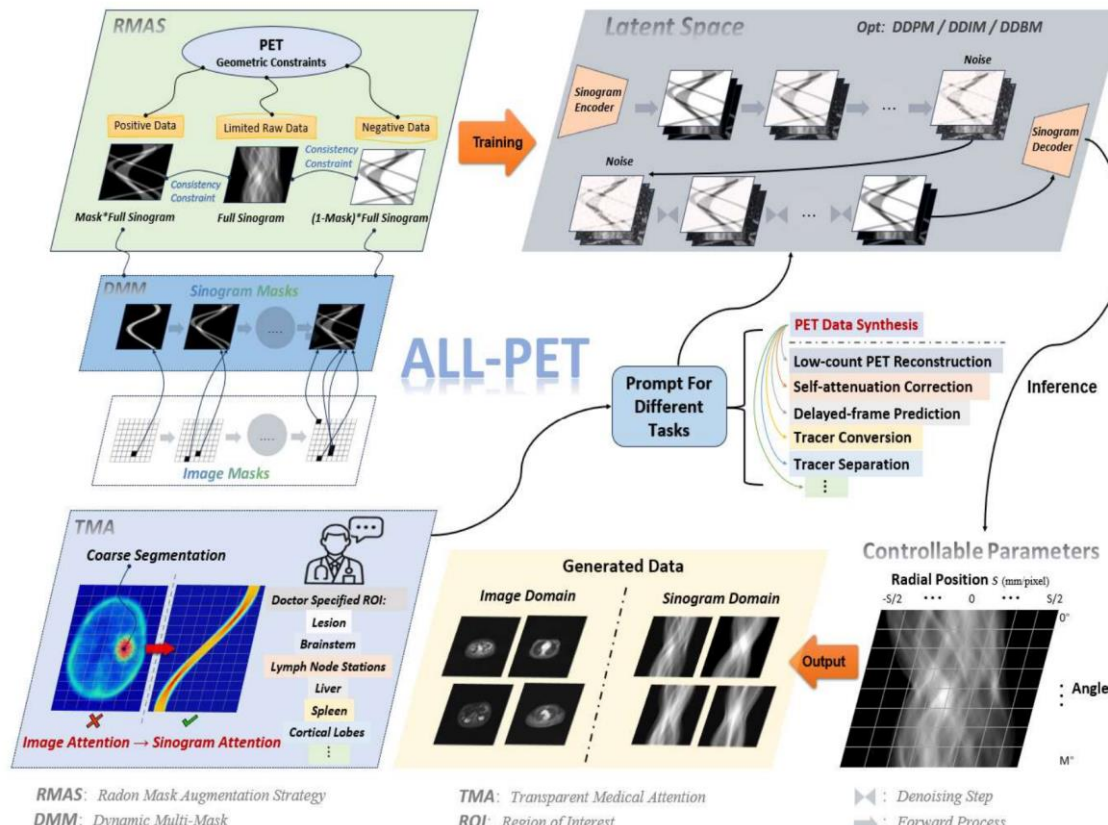
Method	DDPM	U-Net	CycleGAN	ViT	UniSino
Sparse-view	43.156 / 87.110 / 0.0070	43.987 / 98.701 / 0.0062	27.973 / 91.267 / 0.0436	31.376 / 71.241 / 0.0270	48.938 / 97.331 / 0.00353
Limited-angle	21.549 / 74.661 / 0.0837	26.779 / 86.912 / 0.0445	14.533 / 54.136 / 0.1936	12.237 / 43.238 / 0.2444	39.794 / 93.237 / 0.01141
Low-dose	41.689 / 98.170 / 0.0082	45.736 / 98.260 / 0.0051	40.153 / 93.686 / 0.0098	35.172 / 82.611 / 0.0174	49.420 / 97.305 / 0.00335
Down-sample	44.385 / 91.170 / 0.0060	44.798 / 98.640 / 0.0057	40.605 / 93.593 / 0.0093	34.736 / 83.712 / 0.0183	47.567 / 95.091 / 0.00373
Ring	43.483 / 95.590 / 0.0067	41.242 / 97.500 / 0.0086	32.898 / 93.709 / 0.0235	35.468 / 83.591 / 0.0169	49.266 / 97.290 / 0.00341
Truncation	42.400 / 96.712 / 0.0076	37.049 / 92.311 / 0.0141	22.364 / 74.079 / 0.0755	22.821 / 69.116 / 0.0723	42.867 / 96.391 / 0.00794
Geometric	41.690 / 94.202 / 0.0082	37.705 / 95.702 / 0.0128	13.259 / 38.852 / 0.2202	23.355 / 59.036 / 0.0680	40.800 / 97.262 / 0.00912

研究内容

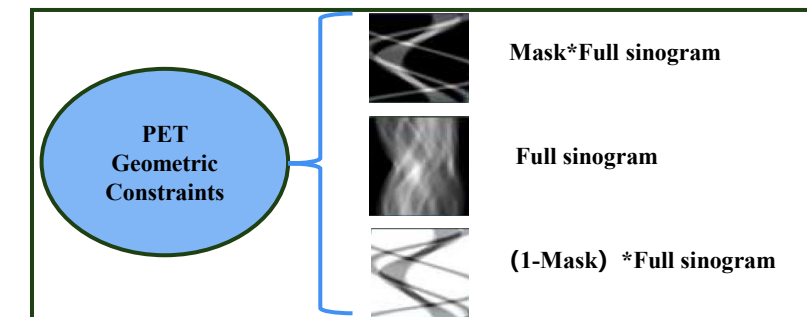
ALL-PET

ALL-PET: A Low-resource and Low-shot PET Foundation Model in Projection Domain

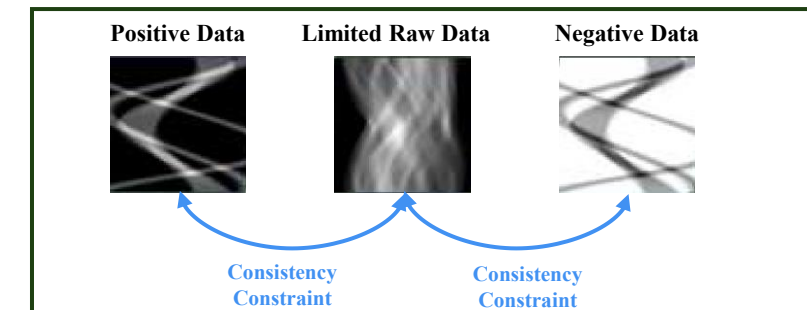
投影域Radon掩码增强的低资源、低样本PET成像基础模型



标注数据获取受限



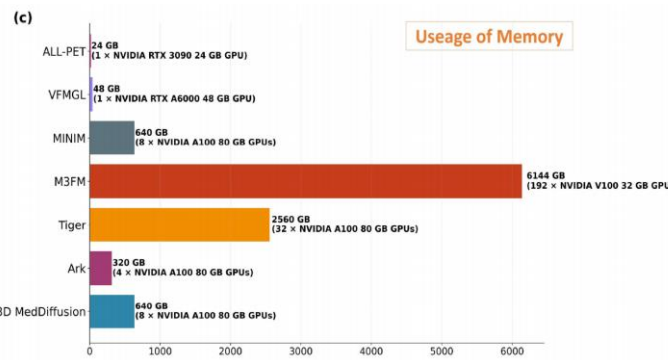
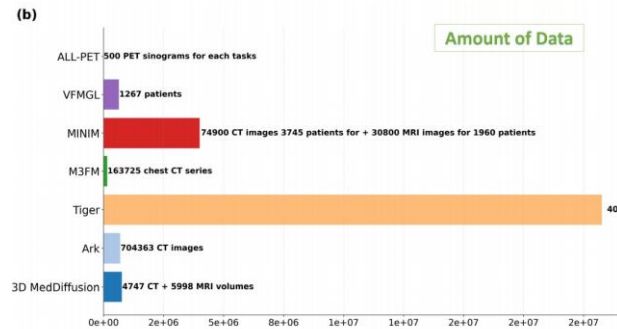
计算资源不足



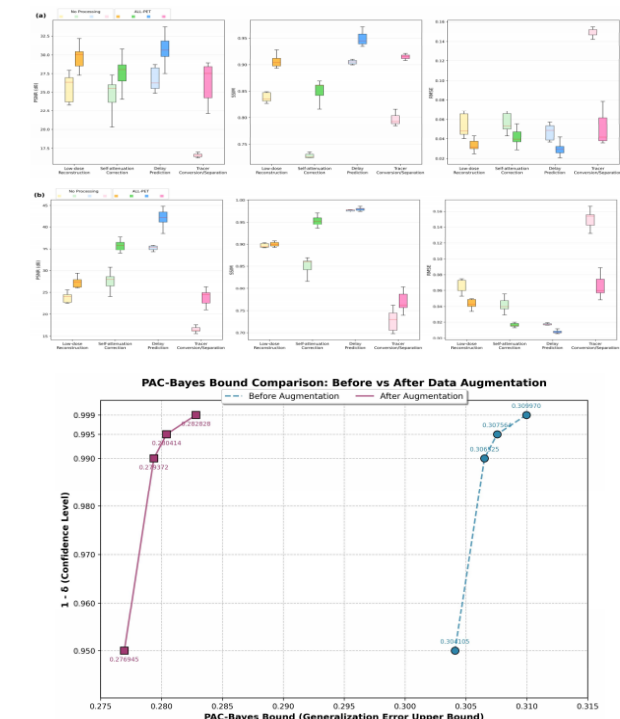
研究内容

ALL-PET ALL-PET: A Low-resource and Low-shot PET Foundation Model in Projection Domain

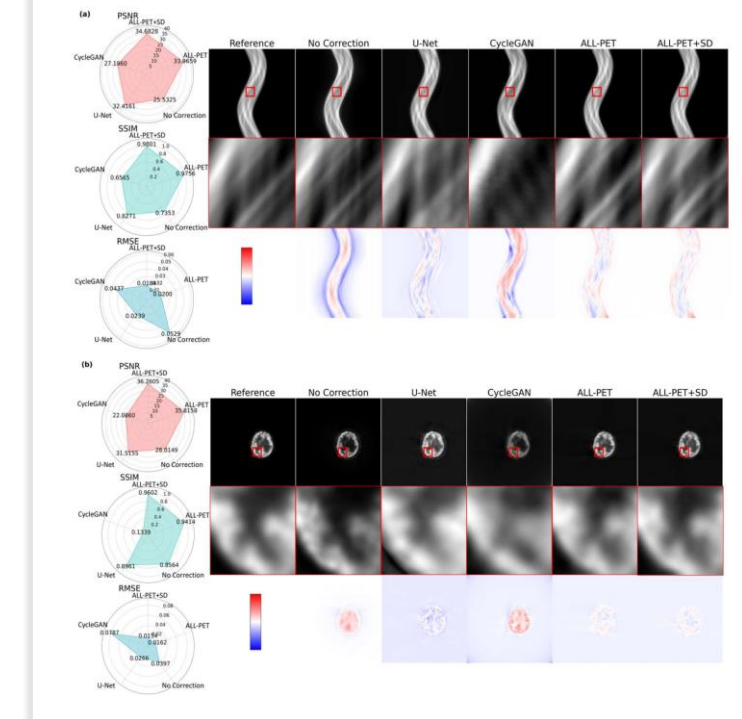
更低的资源占用



更高的性能



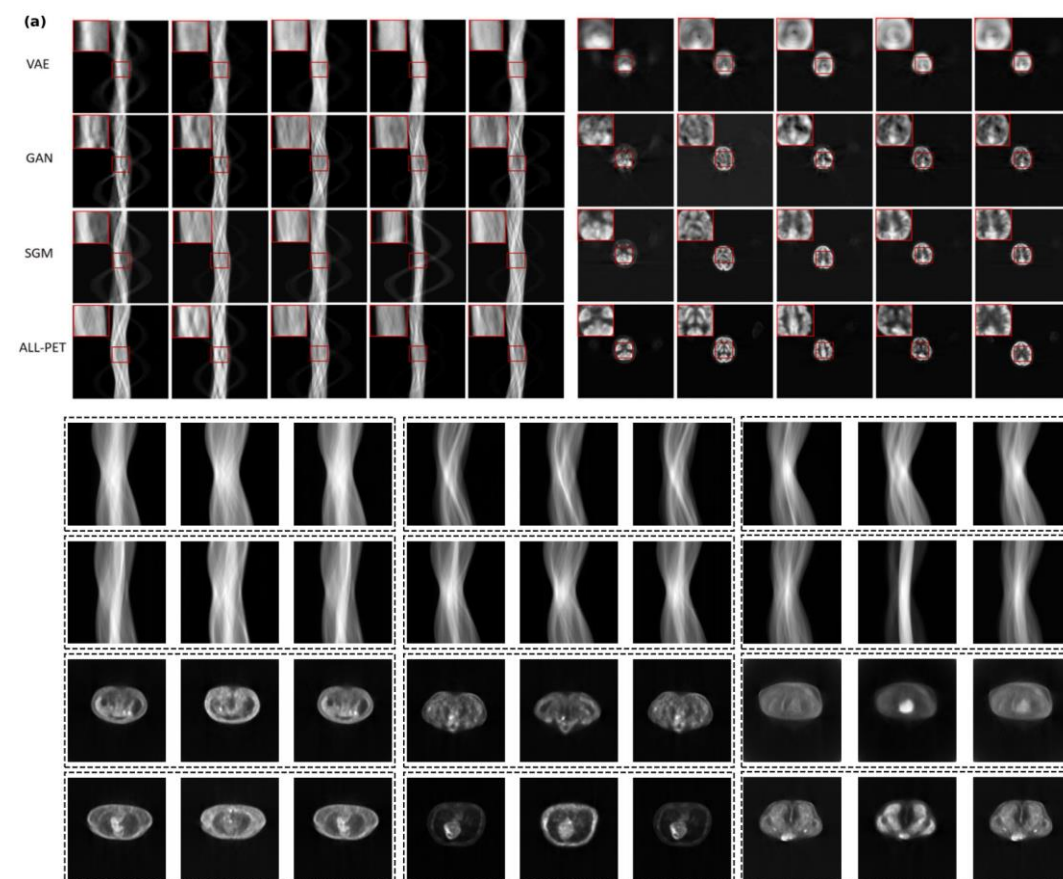
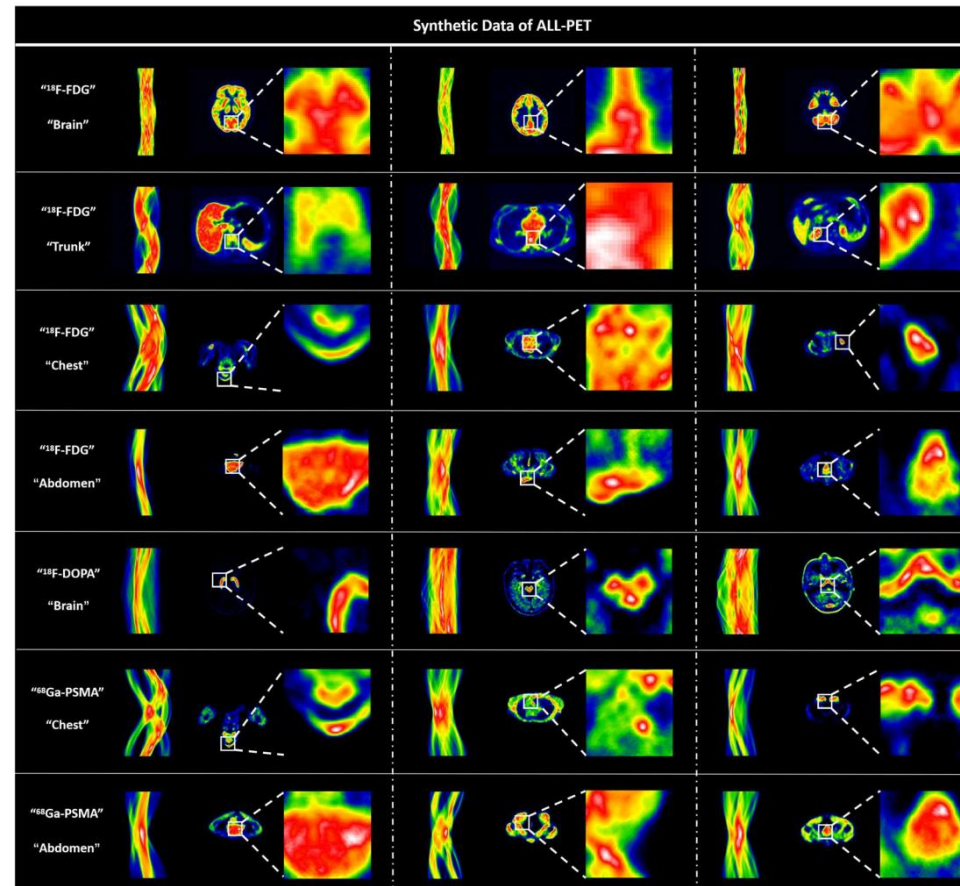
更广泛的应用



研究内容

ALL-PET

ALL-PET: A Low-resource and Low-shot PET Foundation Model in Projection Domain

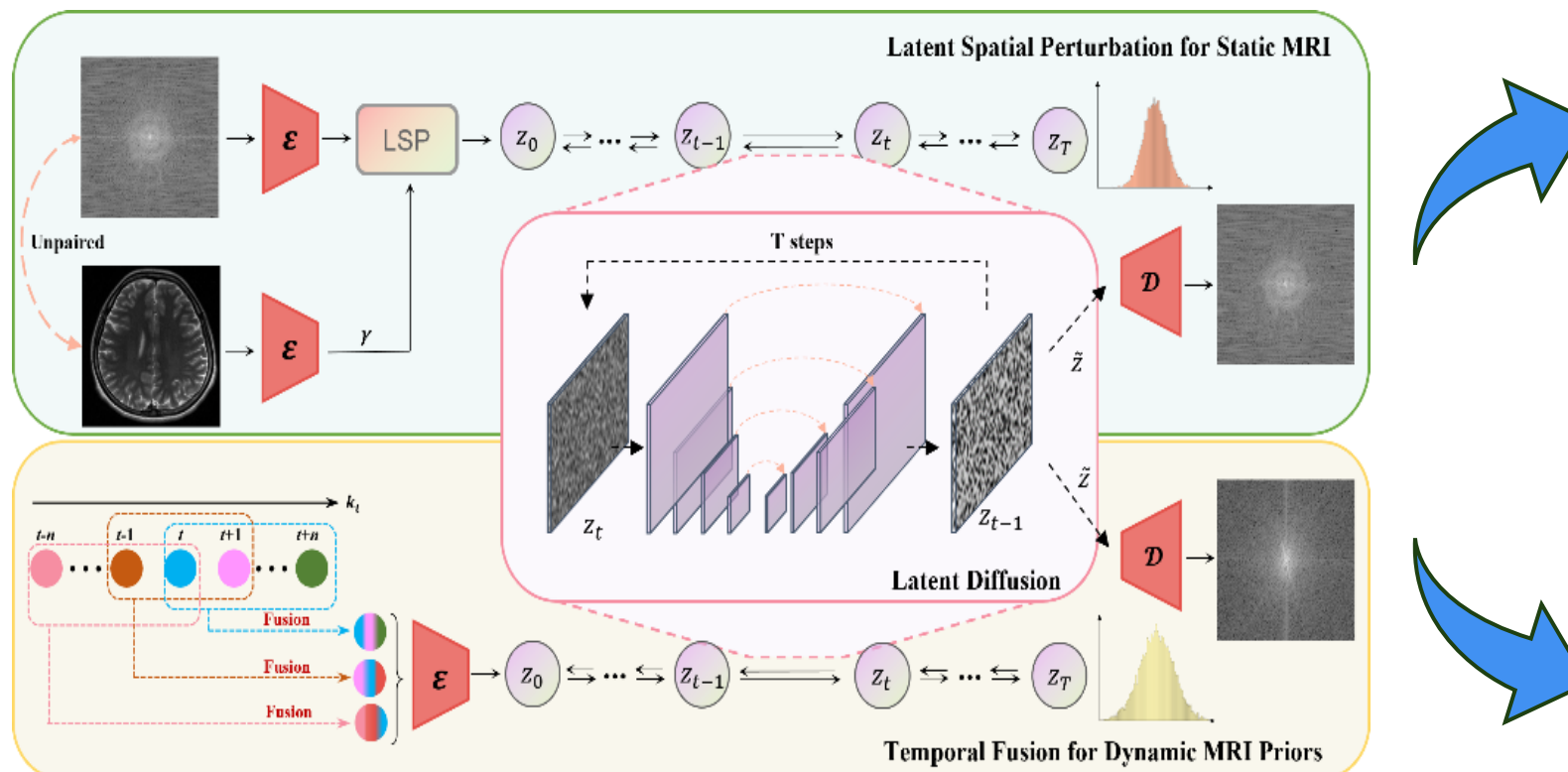


研究内容

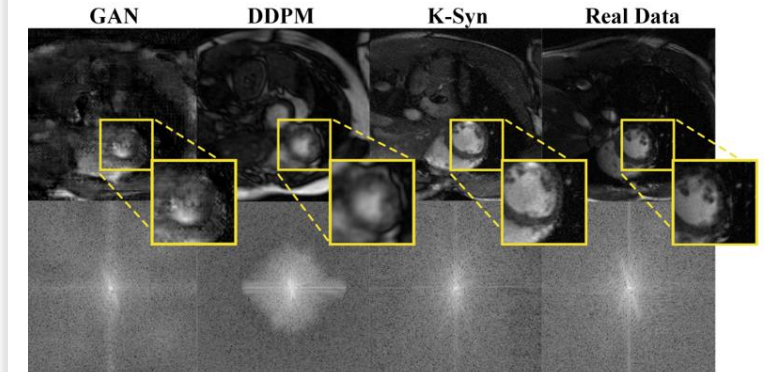
K-Syn

K-Syn: Scenario-Adaptive K-space Data Synthesis via Foundation Model for Data-Scarce MRI Reconstruction

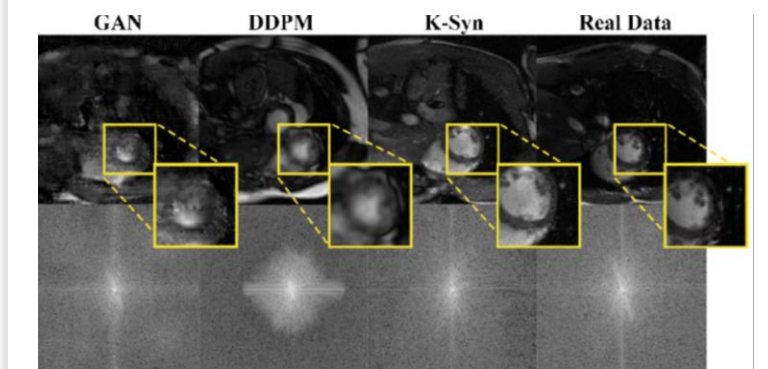
场景自适应的MRI K空间数据合成基础模型



静态：弱监督潜在空间扰动



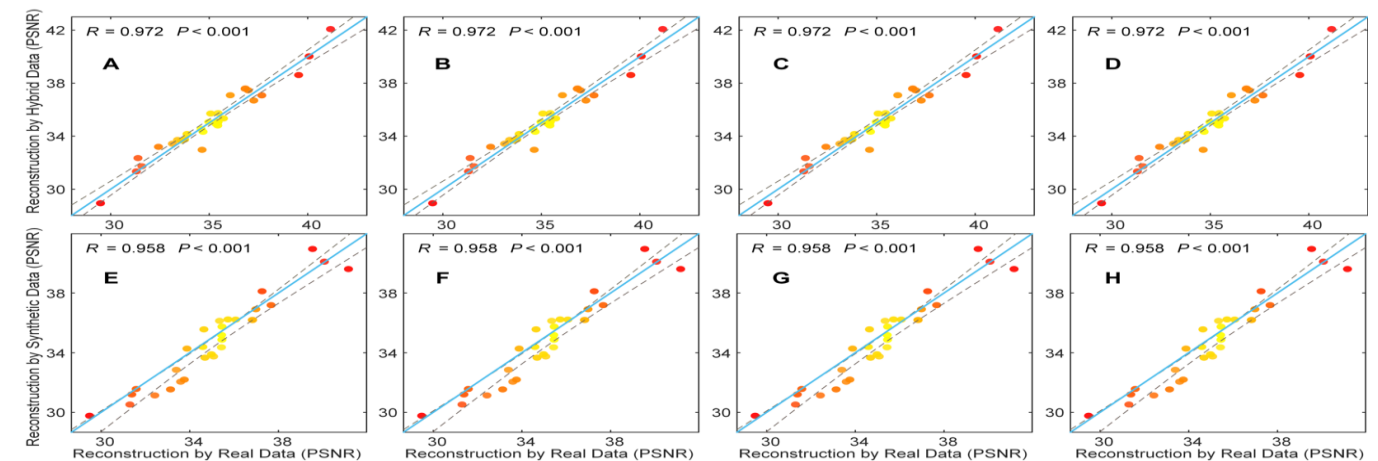
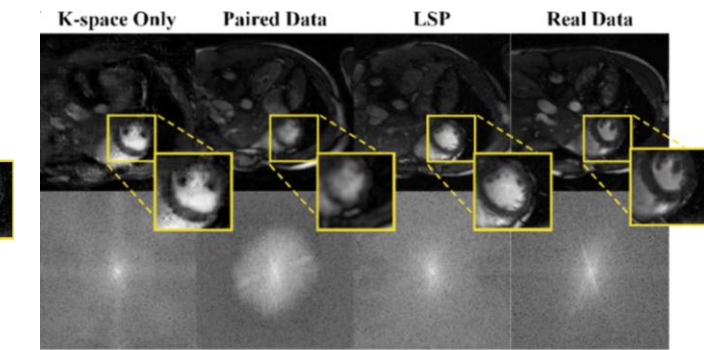
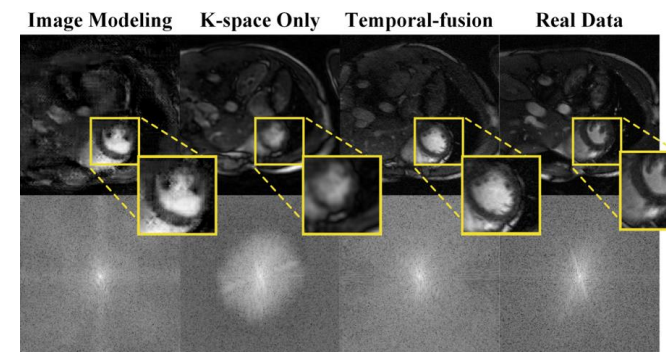
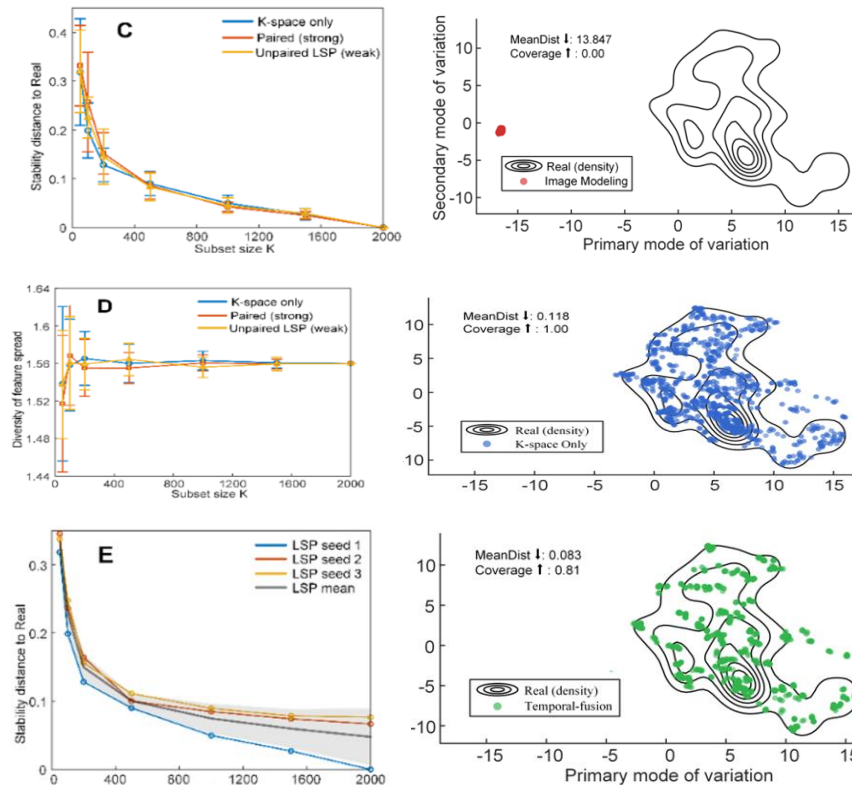
动态：频域特征时间融合





K-Syn

K-Syn: Scenario-Adaptive K-space Data Synthesis via Foundation Model for Data-Scarce MRI Reconstruction





团队成果展示

MR方向

- Correlated and multi-frequency diffusion modeling for highly under-sampled MRI reconstruction. IEEE TMI 2024
- Physics-Informed DeepMRI: K-Space Interpolation Meets Heat Diffusion. IEEE TMI 2024
- One-shot generative prior in Hankel-k-space for parallel imaging reconstruction. IEEE TMI 2023
- Sub-DM: Subspace diffusion model with orthogonal decomposition for MRI reconstruction. IEEE TCI 2026
- Distribution matching with subset-k-space embedding for multi-contrast MRI reconstruction. Medical Physics 2025
- K-Syn: K-space Data Synthesis in Ultra Low-data Regimes. arXiv 2025

- Stage-by-stage wavelet optimization refinement diffusion model for sparse-view CT reconstruction. IEEE TMI 2024
- Dual-domain collaborative diffusion sampling for multi-source stationary computed tomography reconstruction. IEEE TMI 2024

CT方向

- Wavelet-improved score-based generative model for medical imaging. IEEE TMI 2023
- Generative modeling in sinogram domain for sparse-view CT reconstruction. IEEE TRPMS 2023
- UniSino: Physics-Driven Foundational Model for Universal CT Sinogram Standardization. arXiv 2025

PET方向

- RED: Residual estimation diffusion for low-dose PET sinogram reconstruction. Medical Image Analysis 2025
- Low-rank angular prior guided multi-diffusion model for few-shot low-dose CT reconstruction. IEEE TCI 2024
- Diffusion Transformer Meets Random Masks: An Advanced PET Reconstruction Framework. arXiv preprint 2025
- ALL-PET: A Low-resource and Low-shot PET Foundation Model in Projection Domain. arXiv preprint 2025

研究领域：智能成像系统与视觉显示的系统开发与算法研究

- 立足国家大健康战略需求和江西省电子信息产业发展
- 聚焦光电成像系统、软硬件嵌入式开发、信号及视觉处理等行业
- 围绕“传感成像-信号处理-增强显示”中的关键问题与技术瓶颈
- 实现关键技术突破与成果转化



刘且根 教授
国家优青
执行院长
政府津贴获得者



张明辉



徐晓玲



宋贤林 宋文博



万文博



单文哲



官瑜



施柳



肖书源



刘婷婷



吴天涯



王少宇 邹响红

实验室平台及网站：

江西省先进信号处理与智能通信重点实验室

江西省智能医学信息检测与物联网工程研究中心

<https://github.com/yqx7150>; <https://www.labxing.com/lab/1018>



Qiegen Liu
yqx7150

Overview Repositories 124 Projects Pack

Pinned

Diffusion-Models-for-Medical-Imaging Public

Diffusion Models for Medical Imaging

☆ 40 ♂ 2

MLDM Public

Multi-phase FZA Lensless Imaging via Diffusion Model

Python ☆ 8 ♂ 1

<https://github.com/yqx7150>



诚招博士后

WELCOME TO JOIN US

虚位以待 诚聘精英

为吸引国内外优秀博士从事博士后研究工作，培养一批有志于从事生物医学成像、计算光学成像、视觉显示与信息处理等多学科交叉融合研究的优秀青年科研人才，刘且根教授团队依托南昌大学信息工程学院，以国家重点研发计划、国家自然科学基金、企业横向委托项目等为依托，面向国内外诚聘优秀博士后人员（师资博士后、全职博士后、联培博士后）。



观测域医学成像与生成—— 从多分布到多任务

欢迎各位专家指导工作！

官瑜 刘且根

张明辉、徐晓玲、王少宇、施柳、黄彬、房建成、艾星宇、耿梦晓、周泽坤、陈康

